NASA TECHNICAL NOTE

NASA TN D-5236

NASA TN D-5236

ANALYTICAL INVESTIGATION OF AN INFLATABLE LANDING SYSTEM HAVING OMNIDIRECTIONAL AND MULTIPLE-IMPACT CAPABILITIES

by John R. McGehee, Melvin E. Hathaway, and Cornelia B. Dexter

Langley Research Center
Langley Station, Hampton, Va.

NATIONAL AERONAUTICS AND SPACE ADMINISTRATION • WASHINGTON, D. C. • MAY 1969

ANALYTICAL INVESTIGATION OF AN INFLATABLE LANDING SYSTEM HAVING OMNIDIRECTIONAL AND MULTIPLE-IMPACT CAPABILITIES

By John R. McGehee, Melvin E. Hathaway, and Cornelia B. Dexter

Langley Research Center
Langley Station, Hampton, Va.

NATIONAL AERONAUTICS AND SPACE ADMINISTRATION

For sale by the Clearinghouse for Federal Scientific and Technical Information
Springfield, Virginia 22151 – CFSTI price $3.00

ANALYTICAL INVESTIGATION OF AN INFLATABLE LANDING SYSTEM HAVING OMNIDIRECTIONAL AND MULTIPLE-IMPACT CAPABILITIES

By John R. McGehee, Melvin E. Hathaway,
and Cornelia B. Dexter
Langley Research Center

SUMMARY

The use of instrumented probes in the conduct of early planetary exploration will in most instances require survivable landings of these probes on the surfaces of the planets. Because of inadequate data on the atmospheres and surface structures of the planets, a landing system having omnidirectional, multiple-impact, and kinetic-energy-dissipating capabilities could enhance the probability of mission success.

The landing characteristics of a 20-compartment spherical-gas-bag landing system have been investigated for an impact normal to a smooth surface. An analysis was derived and programed for machine computation. Calculations were made to indicate the omnidirectional, multiple-impact, and kinetic-energy-dissipating capabilities over a wide range of ambient pressures.

The results of the computations are presented and show that this landing system has omnidirectional and multiple-impact capabilities. With proper design the system can dissipate 80 to 90 percent of the touchdown kinetic energy during the first impact. The computed results also indicate that this system may be designed to dissipate substantially the entire landing kinetic energy after two impacts. The ability of this landing system to perform satisfactorily over a wide range of ambient pressures has also been demonstrated through computations for landings of a selected vehicle.

INTRODUCTION

The use of instrumented probes in the conduct of early planetary exploration will in most instances require survivable landings of these probes on the surfaces of the planets. Because of inadequate data on the atmospheres and surface structures of the planets, a landing system having omnidirectional, multiple-impact, and kinetic-energy-dissipating capabilities could enhance the probability of mission success. The landing system must also be compatible with the launch and transporting systems. These systems are very

sensitive to mass and volume of the lander vehicle. The gas-bag-type landing system can be stowed in a relatively small volume and holds promise of a small mass as compared with the masses of other types of landing systems which meet the omnidirectional, multiple-impact, and kinetic-energy-dissipating requirements.

Gas-bag landing systems have been investigated and used by the military services for the aerial delivery of cargo (refs. 1 and 2). The Mercury spacecraft were equipped with an air-bag system for shock attenuation during landings (ref. 3). The use of spherical gas bags as omnidirectional landing systems has been proposed in references 4 and 5. These references (refs. 4 and 5) present analyses of the impact motion and the gas dynamics of inflated-sphere landing vehicles. The gas bags analyzed in these papers are uncompartmented; hence, they dissipate little energy internally. Instead, their kinetic energy is dissipated either by bag blowout (single impact) or by friction as the vehicle bounces and rolls on the landing surface (multiple impact). The latter means of energy dissipation is undesirable because the vehicle generally must undergo a large number of impacts, each of which heightens the possibility of damage to landing system and payload.

A compartmented-gas-bag landing system has the advantage of kinetic-energy dissipation through internal gas flow and a resulting decrease in the number of impacts. The results of an experimental and analytical investigation of such a system are reported in reference 6. That investigation, which utilized a simplified test vehicle having unidirectional (vertical-cylinder) gas bags, demonstrated the internal-energy-dissipation capabilities of a compartmented-gas-bag landing system, as well as the utility of an impact analysis that incorporated in an approximate manner the main effects of the internal gas compression cycles and their role in decelerating the landing vehicle.

A compartmented-spherical-gas-bag landing system which in theory possesses the additional capability of omnidirectional impact was proposed in reference 6. Because the spherical gas bag represents a drastic change in geometry, relative to the vertical-cylinder gas bags, an analysis reflecting these geometrical changes is developed herein. This analysis is then used to investigate the landing characteristics of a 20-compartment spherical gas bag during an impact normal to a smooth surface. The programed equations of the analysis have been employed to compute the landing characteristics of a selected vehicle, with particular attention being given to the omnidirectional, multiple-impact, and kinetic-energy-dissipating capabilities of the landing system and, to a limited extent, the operation of the system as related to early planetary exploration.

SYMBOLS

The units used for the physical quantities defined in this paper are given both in the International System of Units (SI) (ref. 7) and in U.S. Customary Units. Appendix A presents factors relating these two systems of units.

A area, meters^2 (feet^2)

A', B', C' angles of spherical triangle forming outer cover of each gas-bag compartment, degrees

a', b', c' angles subtended at center of sphere by arcs opposite A', B', and C', degrees

B flow direction indicator, $\frac{P - p}{|P - p|}$

$D' = \frac{1}{2}(A' + B' + C')$

F decelerating force, newtons (pounds force)

g earth gravitational acceleration, 9.81 meters/second^2 (32.2 feet/second^2)

H constant of proportionality, 1 for SI (32.1739 for U.S. Customary System)

K mass per unit area per ply of material, kilograms/meter^2 (ounces/yard^2)

M_I mass of inner-envelope gas-bag material, kilograms (slugs)

M_O mass of outer-envelope gas-bag material, kilograms (slugs)

M_W mass of gas-bag wall material, kilograms (slugs)

M_T total mass of inner-envelope, outer-envelope, and wall gas-bag material, kilograms (slugs)

$M_{T'}$ total mass of compartmented-gas-bag material including seam allowance, kilograms (slugs)

m mass of gas, kilograms (slugs)

$m_{\ell S}$ landing-system mass, kilograms (slugs)

m_V vehicle mass (payload mass + landing-system mass), kilograms (slugs)

n number of walls in gas bag

P	pressure in receiving reservoir, newtons/meter^2 (pounds force/foot^2)
p	pressure in discharging reservoir, newtons/meter^2 (pounds force/foot^2)
Q	mass flow rate, kilograms/second (slugs/second)
R	gas constant, 287 joules/kilogram-^{o}K (53.3 foot-pounds force/pounds mass-^{o}R)
r	radius, meters (feet)
S_b	surface area of spherical gas bag, meters^2 (feet^2)
S_Δ	area of spherical triangle forming outer cover of each gas-bag compartment, meters^2 (feet^2)
t	time, seconds
Δt	incremental time, seconds
V	volume, meters^3 (feet^3)
y	stroke (vertical displacement of the system center of mass from its position at the initial instant of contact with the surface), meters (feet)
Δy	incremental stroke, meters (feet)
$\dot{y}$	velocity, meters/second (feet/second)
$\ddot{y}$	deceleration, meters/second^2 (feet/second^2)
$\alpha, \theta, \sigma, \phi$	angles defined in appendix B (see sketches 3 and 5), degrees
ρ	mass density of gas, kilograms/meter^3 (slugs/foot^3)

Subscripts:

a	ambient
b	gas bag

c	compressed
e	exhausted
f	footprint
g	gravitational
i	initial
o	orifice
p	payload
t	time interval under consideration
t-1	time interval immediately preceding interval under consideration
w	per wall
y	stroke
1,2,3,4,5,6	quantities in those compartments of the gas bag subjected to identical instantaneous conditions and presented numerically in the order of their association with the landing surface
I,II,III	regimes of stroke

Superscript:

k	ratio of specific heat of gas, 1.4 for air

ASSUMPTIONS AND GEOMETRIC CONSIDERATIONS

In order to obtain an indication of the capabilities of a compartmented-spherical-gas-bag landing system, an approximate mathematical model was derived and programed for machine computation. From this analysis it is possible to determine how various factors such as vehicle mass, bag geometry, initial internal pressure, pressurizing gas, orifice design, external pressure, and impact velocity affect deceleration, jerk (rate of

change of deceleration with time), compartment-pressure rise, gas mass flow between compartments, and kinetic-energy dissipation.

Assumptions

The following assumptions are made in the analysis:

(1) All geometry remains fixed except for distortions in the plane of the landing surface.

(2) The gas-pressure forces are the only forces causing deceleration; friction, bag bending resistance, and the impulsive force required to stop the bag material as it contacts the landing surface are neglected.

(3) During any impact the gas is compressed and expanded in a reversible adiabatic process, and equilibrium conditions exist at each instant.

(4) Because the bag material and the gas represent a small fraction of the total mass of the system, the center of mass of the entire system is taken to be coincident with the center of mass of the payload during as well as before impact.

(5) The impact velocity is limited to values below 100 m/sec (330 ft/sec).

(6) The vehicle impact is normal to the landing surface.

(7) The landing surface is flat, smooth, and rigid.

Geometric Configuration

The configuration employed in this analysis consists of a compartmented spherical gas bag surrounding a spherical payload which is supported with the geometric center of the payload at the geometric center of the spherical bag (fig. 1). The gas bag is divided into 20 identical, radially oriented compartments (compartmented regular icosasphere) and the compartments are interconnected by orifices in the compartment walls. All orifices have the same area. An exploded view of the configuration is shown in figure 2.

The impact characteristics of the spherical bag are functions of the point of impact on the surface of the bag. An analysis of the impact at a random point on the surface of the bag would be a formidable, time-consuming task. However, major changes in gas compression and flow, which are functions of the compartment geometry, should occur for impacts at three typical points on the surface of the spherical bag. These points are labeled in figure 3 as (1) the juncture of five compartments, (2) the center of the arc defined by the intersection of a compartment wall with the outer cover, and (3) the center of the face of one compartment. From a consideration of the orifice area per compartment volume, which roughly defines the pressure change due to gas flow at a given stroke y for each of the impact points, it would appear that the extremes of the variation

of the impact parameters would occur for impacts at the juncture of five compartments and in the center of the face of one compartment. Consequently, impacts at these two points were investigated. In the following discussions of the geometry for these two impact points, it is assumed that no changes in bag geometry occur above the plane of the landing surface. The crushed portion of the bag is assumed to be coincident with the landing surface.

Impact at a juncture of five compartments.- The compartment geometry, the effect of stroke on compartment distortion, and the effect of stroke on the footprint-area patterns are shown in figure 4 for an impact on the surface of the bag at a juncture of five compartments. An impact at this point, because of compartment symmetry, results initially in the compression of five compartments (labeled 1 in fig. 4(a) and referred to as volume 1), with gas flow through five orifices into a second set of five compartments (labeled 2 in fig. 4(a) and referred to as volume 2). The gas mass transfer from volume 1 to volume 2 results in a pressure rise in volume 2, with accompanying gas flow through 10 orifices into a third set of five compartments (labeled 3 in fig. 4(a) and referred to as volume 3). This gas mass transfer from volume 2 to volume 3 causes a pressure rise in volume 3 which initiates gas flow through five orifices into a fourth and final set of five compartments (labeled 4 in fig. 4(a) and referred to as volume 4).

The distortion of the bag by the landing surface is divided into three regimes of stroke (see fig. 4(b)). Regime I includes those values of stroke which result in the distortion of volume 1 from initial contact to the beginning of distortion in volume 2; regime II includes the values of stroke from the beginning of distortion in volume 2 to the beginning of distortion in volume 3; and regime III includes values of stroke from initiation of distortion in volume 3 to the maximum available stroke $(r_b - r_p)$. The sketches in figure 4(c) show the footprint-area patterns associated with each of the regimes of stroke with the footprint area (area of the gas bag in contact with the landing surface) represented by shading. In regime I the compartments in volume 1 are involved; the first sketch shows the footprint-area pattern for the maximum stroke of regime I. In regime II, compartments in volumes 1 and 2 are involved in the footprint-area pattern, which is shown in the second sketch for the maximum stroke of regime II. The sketch for regime III shows that the compartments in volumes 1, 2, and 3 are involved in the footprint-area pattern, and the geometric forms of the footprint areas of each of the compartments in volumes 1, 2, and 3 are shown for the maximum available stroke of this configuration.

Impact at the center of the face of one compartment.- Compartment geometry, the effect of stroke on compartment distortion, and the effect of stroke on the footprint-area patterns are shown in figure 5 for an impact in the center of the face of one compartment. Impact at this point results initially in the compression of one compartment (labeled 1 in

fig. 5(a) and referred to as volume 1), with gas flow through three orifices into a set of three compartments (labeled 2 in fig. 5(a) and referred to as volume 2). The pressure rise in volume 2 due to gas mass transfer from volume 1 results in a flow from volume 2 through six orifices into a set of six compartments (labeled 3 in fig. 5(a) and referred to as volume 3). Simultaneously gas flows from volume 3 through six orifices into a set of six compartments (labeled 4 in fig. 5(a) and referred to as volume 4). Flow is initiated from volume 4 through six orifices into a set of three compartments (labeled 5 in fig. 5(a) and referred to as volume 5). Then gas flows from volume 5 through three orifices into one compartment (labeled 6 in fig. 5(a) and referred to as volume 6).

The distortion of the bag by the landing surface is divided into the three regimes of stroke as defined in the discussion of the impact at a juncture of five compartments. These regimes are identified in the sketches of figure 5(b) in terms of the strokes initiating each of the regimes. The sketches of figure 5(c) show the footprint-area patterns for the compartments involved in each of the three regimes.

ANALYSIS AND COMPUTATIONS

The impact analysis of the compartmented-spherical-gas-bag landing system is formulated by combining the gas equations, auxiliary equations derived from geometric considerations, and equations of motion. Time histories of deceleration, velocity, stroke, and pressure can be obtained from the simultaneous solution of these equations by a numerical integration procedure assuming equilibrium conditions at each instant.

Analytical Procedure

The equations of motion, the pertinent gas equations, and the required geometric equations are presented for an impact normal to the landing surface. The following approximate force-balance equation can be written:

$$m_v\ddot{y} + m_v g \cong (P_b - P_a)A_f \tag{1}$$

The first term in equation (1) represents the inertial force of the vehicle during deceleration. The second term represents the gravitational force. The third term represents the decelerating force due to the pressure in the bag and the area of the bag in contact with the landing surface. The approximation indicated in equation (1) results from the omission of frictional forces, bag bending forces, and the impulsive force required to stop the mass of skin and compartment walls in contact with the landing surface. However, equation (1) is conservative on stroke; that is, the stroke computed from the analysis is greater than that which would be computed if the impulsive ground force were included. Since the

mass of the skin stopped by the ground, for applications considered, is only a small part of the total mass, the equation is not unduly conservative on stroke. Solved for the deceleration, equation (1) becomes

$$\ddot{y} = \left(P_b - P_a\right)\frac{A_f}{m_v} - g \tag{2}$$

Equation (2) can be solved simultaneously with the gas laws and the applicable geometric equations to obtain time histories of deceleration, velocity, stroke, and pressure during an impact.

The gas laws must be employed to predict the pressure rise due to bag distortion and the gas mass transfer due to flow through the orifices. Under actual conditions the gas is compressed and expanded through polytropic processes. However, because of uncertainties in defining the polytropic exponents and in order to simplify the analysis substantially, a reversible adiabatic process is assumed. For a reversible adiabatic process, the pressure-density relation $\frac{P}{\rho^k}$ is constant for each compartment. Substantial dissipation of the vehicle-impact kinetic energy when using a gas-bag landing system requires exhaustion of the gas from the bag either into the atmosphere or into a reservoir which is not directly in contact with the landing surface. Consequently, an analysis of such a system must include gas flow equations. Reference 8 presents equations for the weight flow rate of air through sharp-edged orifices for both subcritical and critical flow conditions. Modified forms of these equations are presented here. For subcritical flow conditions $\frac{P}{p} \geqq 0.53$,

$$Q = 0.465 A_o \sqrt{\frac{Rp\rho}{H}\left(1 - \frac{P^2}{p^2}\right)} \tag{3}$$

For critical flow conditions $\frac{P}{p} < 0.53$,

$$Q = \left(0.449 + 0.241\,\frac{P}{p}\right) A_o \sqrt{\frac{Rp\rho}{H}\left(1 - \frac{P}{p}\right)} \tag{4}$$

As previously noted, these equations were determined from experiments using air. However, reference 9 states that the equations could probably be used for other gases without the introduction of serious error.

The geometric equations which define the footprint area and the volume change due to bag distortion by the landing surface are functions of the point of impact on the surface of the spherical bag. The equations defining these parameters are presented in appendix B for impacts occurring on the surface of the sphere at a juncture of five compartments and in the center of the face of one compartment.

The numerical integration procedure employed for the simultaneous solution of the equations of this analysis is based upon the selection of an incremental time interval which is sufficiently small so that the pressure and density of the gas at the beginning of any time interval may be taken as the average values during the interval. For a given configuration, impact velocity, and acceleration, the assumed time interval can be used in the following equation to compute an incremental stroke:

$$\Delta y_t = \dot{y}_t \, \Delta t + 0.5\ddot{y}_t(\Delta t)^2 \tag{5}$$

The stroke is obtained by summing the incremental strokes and is used in conjunction with applicable geometric equations to compute volume change and footprint area. The volume change, the adiabatic pressure-volume relation, and the gas mass flow equations (which retain only the first term of the Taylor's series expansions) determine an instantaneous value of pressure within each of the volumes of the compartmented bag. These instantaneous values of pressure and the associated instantaneous values of footprint area are substituted into equation (2) to compute an instantaneous value of deceleration. This deceleration, in turn, is used in the following equation to compute the velocity to be used in equation (5) for repeating the procedure:

$$\dot{y}_t = \dot{y}_{t-1} + \ddot{y}_{t-1} \, \Delta t \tag{6}$$

The numerical integration routine is continued until the maximum rebound velocity is attained. The maximum rebound velocity in conjunction with the known touchdown velocity permits the evaluation of the kinetic-energy-dissipating capabilities of the compartmented-spherical-gas-bag landing system.

The equations used for computing the landing characteristics for impacts at the juncture of five compartments and at the center of the face of one compartment are presented in appendix C.

In order to illustrate the multiple-impact and kinetic-energy-dissipating capabilities of the proposed landing system, certain assumptions were required in programing the equations of the analysis. For that portion of the impact during which the gas-bag landing system is being compressed, the program simply performs operations on the equations in the order presented in appendix C. During the rebound portion of an actual impact, bag

flexibility limits the minimum pressure in any compartment to ambient pressure. However, during rebound the programed equations would give pressures below ambient. The below ambient pressures result since the geometric equations are based on stroke which, because of the rebound velocity, results in a computed geometric volume greater than that which would be occupied by the mass of gas in the compartment at ambient pressure. Thus the program is altered to hold the pressure constant at ambient pressure, and the volume occupied by the gas at ambient pressure at each instant is computed. When gas flow equalizes this volume and the geometric volume, pressure is again computed from the programed equations of appendix C.

Computations

The omnidirectional, multiple-impact, and kinetic-energy-dissipating capabilities of the compartmented-gas-bag landing system were investigated for a selected vehicle. Because this landing system may have application during early planetary exploration, computations for the selected vehicle were made in order to examine the adaptability of the system at various ambient pressures. An estimate of the mass of the gas-bag landing system used in this study is also included. The following landing parameters, representative of those being considered for planetary landing vehicles, were used herein:

Vehicle mass (total landed mass)	230 kilograms (15.735 slugs)
Gas bag radius	0.9 meter (3 feet)
Payload radius	0.3 meter (1 foot)
Orifice radii	0.06 meter (0.21 foot)
Maximum allowable stroke; that is, $0.9(r_b - r_p)$	0.54 meter (1.8 feet)
Payload density	1400 kg/m^3 (2.7 $slugs/ft^3$)
Pressurizing gas	Air
Initial gas pressure	111.5 kN/m^2 (2329 lbf/ft^2)
Touchdown velocity	23 m/sec (75 ft/sec)
Maximum allowable deceleration	2.45 km/sec^2 (8050 ft/sec^2)

RESULTS AND DISCUSSION

The programed equations of the analysis were used to compute time histories of deceleration, velocity, stroke, gas temperatures, and compartment pressures for landings of the selected vehicle subject to the conditions specified in the preceding section. The results of these computations are presented in figures 6 to 8 and are discussed with the intent of illustrating the omnidirectional, multiple-impact, and kinetic-energy-dissipating capabilities of the proposed landing system.

Landing Characteristics and Omnidirectional Capability

To demonstrate the omnidirectional capability of the proposed landing system, computations were made for impacts at the locations on the spherical bag (the juncture of five compartments and the center of the face of one compartment) that result, because of compartment configuration, in extremes in the variation of the impact characteristics. These computations were made with a selected ambient pressure of 101.4 kN/m^2 (2117 lbf/ft^2) and a bag initial pressure of 111.5 kN/m^2 (2329 lbf/ft^2). The results are presented in figure 6.

Figure 6(a) presents time histories of deceleration, velocity, and stroke for impacts on the surface of the spherical gas bag at the juncture of five compartments (juncture impact) and at the center of the face of one compartment (face impact). A maximum deceleration of approximately 195 earth g-units was obtained for the juncture impact and a maximum of approximately 115 earth g-units was obtained for the face impact. As would be expected on the basis of the deceleration results, the stroke for the face impact, 0.55 meter (1.8 feet), was greater than that for the juncture impact, 0.51 meter (1.7 feet). Since the spherical payload is supported with the geometric center of the payload at the geometric center of the spherical gas bag (same available stroke for impact at any point on the spherical gas bag) and since these computations were made for impacts at locations on the spherical bag which represent the extremes of variation of the impact characteristics, the gas bag has omnidirectional capability for the selected values of the parameters.

Time histories of gas temperatures and compartment pressures obtained from computations made for the critical impact points are presented in figure 6(b). Maximum pressure and, consequently, maximum gas temperature occurred for the juncture impact. Hence it appears that designed structural strength of such a system should be based on the impact characteristics obtained for a juncture impact.

Multiple-Impact Capability

The primary question that arises when considering the multiple-impact capability of the proposed gas-bag landing system concerns the time available between impacts for complete recovery of stroke capability. In order to examine the multiple-impact capability of the proposed landing system, computations were made for first and second impacts of the selected vehicle for the critical points of impact. The results of these computations are shown in figure 7. Time histories of deceleration, velocity, stroke, and volume 1 pressure for the first and second impacts of a landing at a juncture of five compartments are shown in figure 7(a). It was assumed that touchdown for both impacts occurred at the juncture of five compartments. Zero stroke in the figure represents the position of the center of gravity at the instant the bag initially contacts the landing

surface. Full stroke capability for a subsequent impact will result when the internal pressure has equalized throughout the gas bag. It was shown in figure 6(b) that the gas pressure in the bag had equalized in all volumes when the volume 1 pressure had returned to the bag initial pressure. Consequently, only volume 1 pressures are shown in figure 7(a). For the first impact, volume 1 pressure had returned to the value of initial bag pressure at a time of approximately 0.12 second and at this time the stroke was approximately -0.16 meter (-0.52 foot). These conditions meet the criteria for recovery of full stroke capability. It is also of interest to note that at the time of recovery of full stroke capability the vehicle had a rebound velocity of 7.5 m/sec (25 ft/sec), the indication being that the gas-bag landing system had recovered and was ready for operation during a subsequent impact.

The results obtained from computations of the first and second impacts for impact at the center of the face of one compartment are shown in figure 7(b). Results from computations for the first impact show that full stroke capability had been recovered while the vehicle was rebounding at a velocity of 10 m/sec (32.8 ft/sec). For the second impact the bag recovered full stroke capability while the vehicle was rebounding with a velocity of 5.9 m/sec (19.4 ft/sec) and hence was capable of operating for subsequent impacts.

The results obtained from the computations of the first and second impacts of the selected vehicle, for the critical points of impact, show that the proposed gas-bag landing system recovers stroke capability between impacts and thus has a multiple-impact capability.

Vehicle-Kinetic-Energy Dissipation

Kinetic-energy dissipation of an actual gas-bag landing system is believed to be achieved as described in the present section. When the inflated sphere strikes a hard surface, the bag deforms to the shape of the surface and gas compression occurs in those compartments in contact with the surface, causing gas to flow through orifices into the uncompressed (storage) compartments. Thus the kinetic energy of the vehicle is transformed into kinetic and increased internal energy of the gas. Because of the restrictive nature of the orifices, the pressure in the compressed compartments increases more rapidly than the pressure in the storage compartments. The force generated by the pressure in the compartments in contact with the surface causes deceleration of the vehicle. When the vehicle velocity has been reduced to zero and rebound begins, gas is still flowing from the compressed compartments to the storage compartments. Thus, there is a phase lag between the internal gas flow cycle and the impact-rebound cycle, so some of the energy of the gas which is stored as heat energy and potential energy in the storage compartments during impact is not available during rebound. As rebound continues, the vehicle loses contact with the surface; then the internal gas flow cycle reverses and the

gas flows from the storage compartments back into the formerly compressed compartments, returning the bag to its spherical shape. In the present analysis the dissipated kinetic energy is assumed to be transformed into heat energy within the gas.

The kinetic-energy-dissipation capability of the proposed landing system is obtained by analyzing the results of computations presented in figures 6 and 7 for landings of the selected vehicle at the critical points of impact. The kinetic energy dissipated is determined by comparing the maximum velocity of rebound after each impact with the initial touchdown velocity of the vehicle. The results in figure 6(a) for the juncture impact show that the maximum rebound velocity is 8.2 m/sec (27.0 ft/sec), which is approximately 35 percent of the touchdown velocity and which corresponds to dissipation of approximately 87 percent of the vehicle touchdown kinetic energy during the first impact. For the face impact the maximum rebound velocity is 10.6 m/sec (34.8 ft/sec), which is approximately 46 percent of the touchdown velocity and which corresponds to dissipation of approximately 79 percent of the vehicle touchdown kinetic energy during the first impact. Therefore, for the selected vehicle and specified landing parameters, the minimum kinetic-energy-dissipation capability during the first impact of a landing should be approximately 80 percent. The values of kinetic-energy dissipation cited do not include energy losses which may result from friction, bag flexing, and impulsive reaction forces.

It is also of interest to obtain an indication of the number of impacts that may be required to dissipate the initial touchdown kinetic energy. The effects of the transformed kinetic energy on the landing characteristics for an impact subsequent to the initial impact are investigated for two conditions. First, it is assumed that all of the transformed kinetic energy or stored heat energy is absorbed by the envelope during rebound and hence, during rebound, the pressure and temperature of the gas return to initial values. Second, it is assumed that the stored heat energy is not absorbed by the envelope during rebound but is reflected in an increase in pressure and temperature of the gas relative to the values existing prior to initial touchdown.

The results of computations for the second impact for a landing of the vehicle under the specified conditions are shown in figure 7. Time histories of stroke, velocity, deceleration, and volume 1 pressure are shown in figure 7(a) as obtained from computations for the second impact at the juncture of five compartments. The initial pressure and temperature of the gas in the bag at second impact were determined for the two conditions previously stated. The values of stroke, velocity, deceleration, and volume 1 pressure for the second impact should lie between the values obtained from these computations. The rebound and subsequent touchdown occur in a short time interval (approximately 1.6 seconds); consequently, very little of the transformed kinetic energy or stored heat energy may be absorbed by the bag envelope. Hence the landing characteristics for the second impact, as determined from the computation assuming that the heat energy is

stored in the gas with no absorption by the bag envelope, should be more representative of an actual landing impact of the system. Under either condition the total kinetic energy dissipated varies by only 3 percent. Similarly, time histories of stroke, velocity, deceleration, and volume 1 pressure were obtained from computations for the first and second impacts at the center of the face of one compartment and are shown in figure 7(b).

The results of the computations for the first and second impacts for landings of the vehicle under the specified conditions show that approximately 90 percent of the initial touchdown kinetic energy has been dissipated at the end of the second impacts. Kinetic energy losses due to friction, bag flexing, and impulsive reaction forces were not included in the analysis; therefore, the computed results indicate that the proposed system may be designed to dissipate substantially the entire kinetic energy during the first two impacts.

Ambient Pressure Environments

The proposed landing system has potential for application in the conduct of early unmanned planetary exploration. Consequently, it may be required to operate over a wide range of ambient pressures. To illustrate this facet of the operational capability of the system, computations for the critical impact points were made for landings of the selected vehicle for a range of ambient pressures from 0 to 3 earth atmospheres. The results of these computations are shown in figure 8 as time histories of deceleration and stroke. Values of initial bag pressure were determined by trial and error so that the maximum values of deceleration and stroke did not exceed values previously specified. A limitation of this procedure is illustrated in figure 8(d) where it can be seen that when the initial bag pressure was assumed equal to the ambient pressure (lower limit for bag deployment), the maximum deceleration for the juncture impact exceeded the specified maximum value of 250 earth g-units. Thus, in order to design a system for operation in an ambient pressure environment of this magnitude and within the specified landing constraints, variation of landing system design parameters other than initial bag pressure would be required. Since the selected vehicle was designed to operate efficiently for an ambient pressure of 1 earth atmosphere and the computed results show that the proposed system performs within the specified constraints over a wide range of ambient pressures, the proposed landing system could be designed for use in unmanned planetary exploration.

Landing System Mass

Landing system mass, although not directly involved in the previous analysis, must be considered in the practical application of this system. A mass analysis is presented in appendix D. For the values of the parameters used, this analysis yields a landing system mass of approximately one-fourth the total landed mass.

CONCLUDING REMARKS

An analytical procedure has been developed for investigating the landing characteristics of a 20-compartment spherical-gas-bag landing system for landings normal to a smooth surface. The results of computations for landings of a selected vehicle employing the spherical-gas-bag system show that the system has an omnidirectional landing capability and a multiple-impact capability. The values of kinetic-energy dissipation computed from the analysis do not include losses that may result from bag flexing, impulsive reaction forces, and so forth. However, with proper design the system should dissipate at least 80 percent of the touchdown kinetic energy during the first impact. The computed results indicate that the proposed system may be designed to dissipate substantially the entire landing kinetic energy during the first two impacts. Since the proposed landing system may have application in early planetary exploration, it must be capable of operating in various ambient pressure environments. The results of computations show that with proper design the landing system can perform satisfactorily over a wide range of ambient pressures.

Langley Research Center,
National Aeronautics and Space Administration,
Langley Station, Hampton, Va., February 24, 1969,
124-08-04-14-23.

APPENDIX A

CONVERSION OF SI UNITS TO U.S. CUSTOMARY UNITS

Conversion factors for the units used herein are given in the following table:

Physical quantity	SI Unit	Conversion factor (*)	U.S. Customary Unit
Length	meters (m)	0.3048	ft
Force	newtons (N)	4.448	lbf
Density	kilograms/cubic meter (kg/m^3)	515.38	$slugs/ft^3$
Pressure	kilonewtons/square meter (kN/m^2)	0.0479	lbf/ft^2
Mass	kilograms (kg)	14.594	slugs
Energy	joules (J)	1.3558	ft-lbf
Mass flow	kilograms/second (kg/sec)	14.594	slugs/sec
Velocity	meters/second (m/sec)	0.3048	ft/sec
Deceleration . . .	meters per sec per sec (m/sec^2)	0.3048	ft/sec^2

*Divide value given in SI Unit by conversion factor to obtain equivalent value in U.S. Customary Unit.

Prefixes to indicate multiple of units are as follows:

Prefix	Multiple
centi (c)	10^{-2}
kilo (k)	10^3
mega (M)	10^6

APPENDIX B

GEOMETRIC EQUATIONS

In this appendix expressions for compressed volume and footprint area for a spherical gas bag having 20 equal-volume, radially oriented compartments are derived for impacts at a juncture of five compartments and at the center of the face of one compartment.

Compartment Geometry

When a sphere is divided into 20 identical, radially oriented compartments, the surface of the sphere is thereby divided into 20 congruent, equilateral spherical triangles. Hence the solution of one of the spherical triangles defines the geometry of all the triangles.

The area of a spherical triangle forming the outer cover of one compartment is

$$S_\Delta = \frac{A' + B' + C' - 180^o}{180^o} \pi r_b^2 \tag{B1}$$

where A', B', and C' are angles of the triangle and r_b is the radius of the sphere. The surface area of the spherical gas bag is

$$S_b = 4\pi r_b^2 \tag{B2}$$

Consequently, the area of one of the spherical triangles is

$$S_\Delta = \frac{S_b}{20} = \frac{\pi r_b^2}{5} \tag{B3}$$

Since the triangle is equilateral,

$$A' = B' = C' \tag{B4}$$

and

$$a' = b' = c' \tag{B5}$$

where a', b', and c' are the angles subtended at the center of the sphere by the arcs opposite the angles A', B', and C', respectively. Hence equation (B1) may be written as

APPENDIX B

$$S_\Delta = \frac{3A' - 180^o}{180^o} \pi r_b^2 \tag{B6}$$

Equating equations (B3) and (B6) and solving for A' yields $A' = 72^o = B' = C'$.

The angles a', b', and c' may be found from

$$\sin \frac{a'}{2} = \sqrt{\frac{-\cos D' \cos(D' - A')}{\sin B' \sin C'}} \tag{B7}$$

where $D' = \frac{1}{2}(A' + B' + C') = 108^o$. Solving equation (B7) for a' gives $a' = 63^o26' = b' = c'$. (See sketch 1.) The length of the sides may be determined from the radius of the sphere and a', b', and c'.

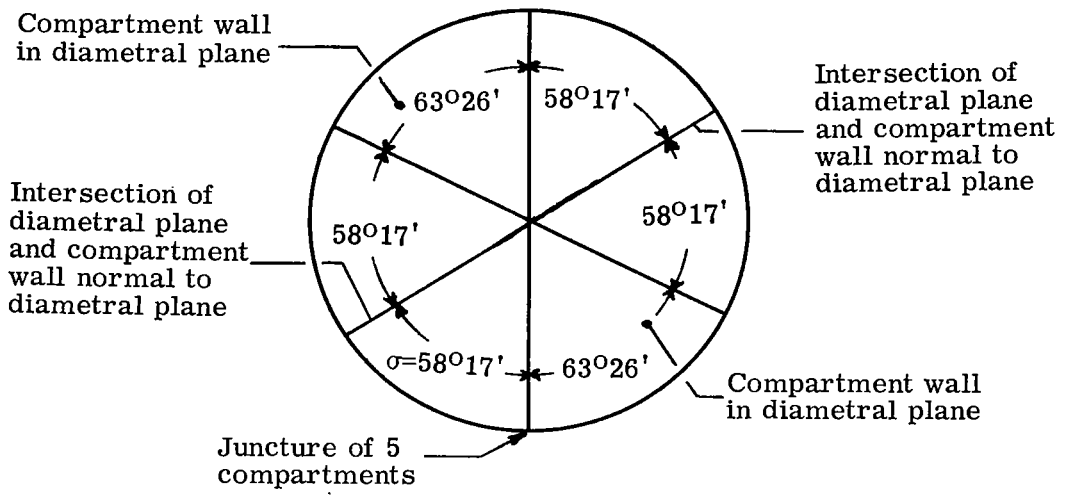

Sketch 1

Because of symmetry of the compartmentation, a diametral plane oriented to contain a compartment wall contains two diametrically opposite compartment walls and bisects two other walls, as shown in sketch 1. The angle σ formed by the line representing the juncture of five compartments and the line defined by the intersection of the diametral plane with a compartment wall normal to the diametral plane may be determined from the equation $4\sigma + 2(63^o26') = 360^o$. The resulting value of σ is $58^o17'$.

Bag Geometry During Impact at a Juncture of Five Compartments

Impact at a juncture of five compartments, for the configuration with 20 equal-volume, radially oriented compartments and an available stroke $(y = r_b - r_p)$ greater

than $r_b(1 - \cos 63^\circ 26')$, could result in volume distortion in three sets of five compartments. The set of five compartments which is first distorted by the landing surface is referred to as volume 1. The second set of five compartments to be distorted by the landing surface during an impact is designated volume 2. The third set of five compartments to be distorted is referred to as volume 3. The fourth set of five compartments is not distorted by the landing surface, but as a result of gas flow serves as a storage volume and is designated volume 4. The geometry of the impact is divided into three regimes based on the value of stroke at which distortion originates in each of the first three volumes. The volumes and regimes defined for an impact at a juncture of five compartments are shown in sketch 2.

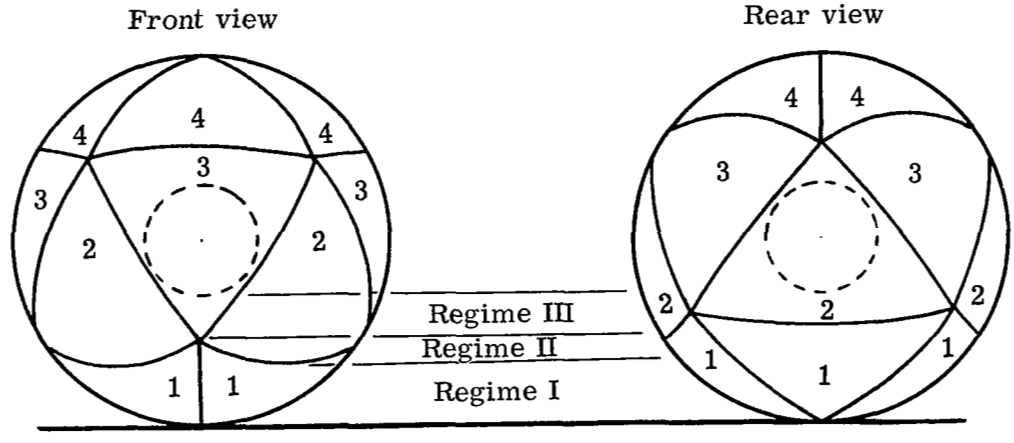

Sketch 2

The following equations for the compressed volume V_c (volume decrease due to distortion of the spherical bag by the landing surface) and for the footprint area A_f are presented as functions of stroke and bag radius for regime I:

$$V_{c,1} = \frac{\pi}{3} y^2(3r_b - y)$$

$$A_{f,1} = \pi(2r_b y - y^2)$$

$$V_{c,2} = 0$$

$$A_{f,2} = 0$$

$$V_{c,3} = 0$$

$$A_{f,3} = 0$$

These equations hold for values of stroke of $0 \leqq y \leqq y_I = r_b - r_b \cos 58^\circ 17'$.

APPENDIX B

The equations for regime II are

$$V_{c,1} = \frac{\pi}{3} y^2(3r_b - y) - V_{c,2}$$

$$A_{f,1} = \pi(2r_b y - y^2) - A_{f,2}$$

$$V_{c,2} = \sum_{y_I}^{y} A_{f,2}\, \Delta y$$

$$A_{f,2} = \frac{5r_f^2}{2}\left(\frac{\pi\theta}{180^o} - \sin\theta\right)$$

$$= \frac{5}{2}(2r_b y - y^2)\left\{\frac{2\pi}{180^o}\cos^{-1}\left(\frac{r_b - y}{\tan 31^o43'\sqrt{2r_b y - y^2}}\right)\right.$$

$$\left. - \sin\left[2\cos^{-1}\left(\frac{r_b - y}{\tan 31^o43'\sqrt{2r_b y - y^2}}\right)\right]\right\} \quad \text{(see sketch 3)}$$

$$V_{c,3} = 0$$

and

$$A_{f,3} = 0$$

These equations are valid for strokes within the limits of

$$r_b - r_b \cos 58^o17' = y_I \leqq y \leqq y_{II} = r_b - r_b \cos 63^o26'$$

The equations for regime III are

$$V_{c,1} = V_{1,i} - V_{1,y} = \frac{\pi}{3}(r_b^3 - r_p^3) - \left[\frac{5 \sin 72^o \tan^2 63^o26'(r_b - y)^3}{6} - \frac{\pi r_p^3}{3}\right]$$

$$A_{f,1} = \frac{5}{2} \sin 72^{o} \tan^{2} 63^{o}26'(r_b - y)^2$$

$$V_{c,2} = \frac{\pi}{3} y^2(3r_b - y) - V_{c,1} - V_{c,3}$$

$$A_{f,2} = \pi(2r_b y - y^2) - A_{f,1} - A_{f,3}$$

$$V_{c,3} = \sum_{y_{II}}^{y} A_{f,3} \, \Delta y$$

and

$$A_{f,3} = 5\left[\frac{cL}{2} + \frac{r_f^2}{2}\left(\frac{\pi\phi}{180^{o}} - \sin \phi\right)\right] \qquad \text{(see sketch 3)}$$

where

$$\frac{c}{2} = r_f \sin \frac{\phi}{2}$$

$$L = \frac{c}{2 \tan \frac{\alpha}{2}}$$

$$r_f = \sqrt{2r_b y - y^2}$$

and

$$\phi = \alpha - 2 \sin^{-1}\left[\frac{(r_b - y)\tan 63^{o}26' \sin \frac{\alpha}{2}}{r_f}\right]$$

For this configuration and impact point, $\frac{\alpha}{2} = \tan^{-1}(\tan 36^{o} \sin 26^{o}34') = 18^{o}$.

The equations for regime III hold for values of stroke of

$$r_b - r_b \cos 63^{o}26' = y_{II} \leqq y \leqq r_b - r_p$$

APPENDIX B

The footprint planes and the elevation view for an impact at a juncture of five compartments are shown in sketch 3.

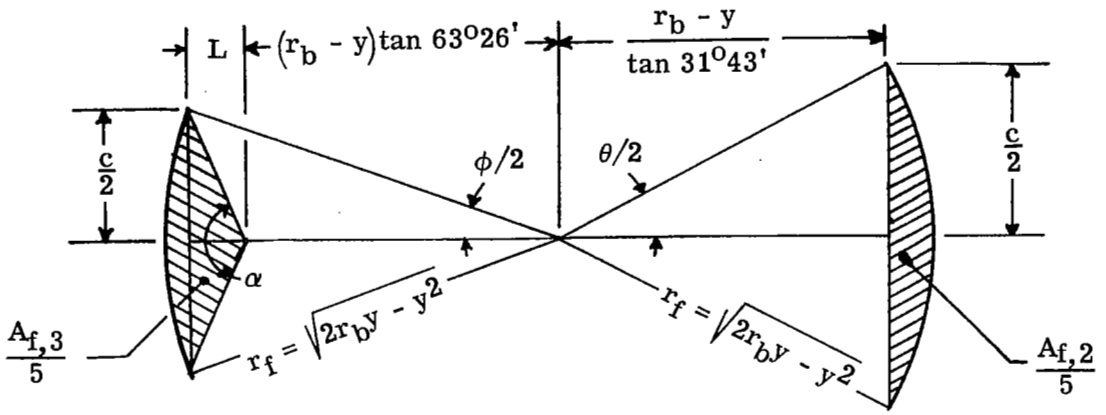

Footprint planes

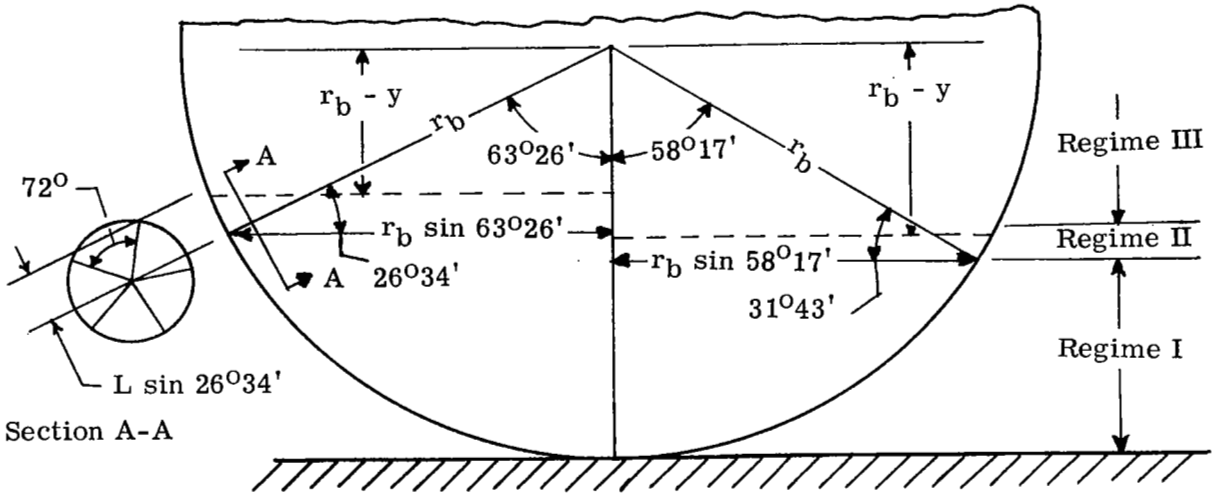

Elevation view

Sketch 3

Bag Geometry During Impact at the Center of the Face of One Compartment

Impact at the center of the face of one compartment may result in volume distortion initially in one compartment (volume 1), then in three additional compartments (volume 2), and finally in six additional compartments (volume 3). The six compartments of volume 4, the three compartments of volume 5, and the one compartment of volume 6 are not subject to distortion by the landing surface during the first impact, but because of gas flow they serve as storage volumes. There are three regimes of stroke, similar to those defined

for the impact at a juncture of five compartments. Sketch 4 shows these volumes and regimes defined for an impact at the center of the face of one compartment.

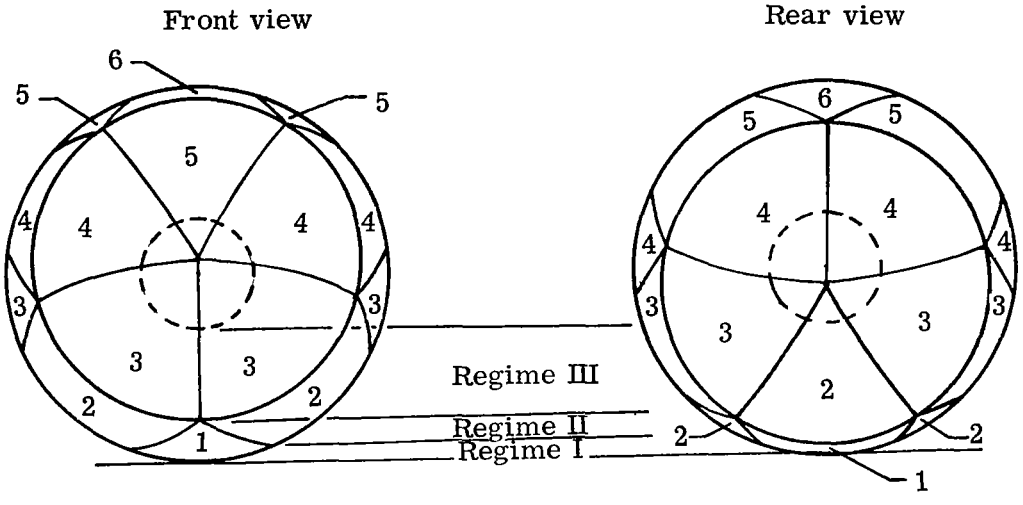

Sketch 4

For regime I the equations for the compressed volume V_c (volume decrease due to distortion of the spherical bag by the landing surface) and the footprint area A_f as functions of stroke and bag radius are

$$V_{c,1} = \frac{\pi}{3} y^2(3r_b - y)$$

$$A_{f,1} = \pi(2r_b y - y^2)$$

$$V_{c,2} = 0$$

$$A_{f,2} = 0$$

$$V_{c,3} = 0$$

and

$$A_{f,3} = 0$$

These equations are applicable for values of stroke of $0 \leqq y \leqq y_I = 0.06580r_b$.

APPENDIX B

The equations for regime II are

$$V_{c,1} = \frac{\pi}{3} y^2(3r_b - y) - V_{c,2}$$

$$A_{f,1} = \pi(2r_b y - y^2) - A_{f,2}$$

$$V_{c,2} = \sum_{y_I}^{y} A_{f,2}\, \Delta y$$

$$A_{f,2} = \frac{3}{2}(2r_b y - y^2)\left\{\frac{2\pi}{180^o} \cos^{-1}\left(\frac{r_b - y}{\tan 69^o6' \sqrt{2r_b y - y^2}}\right)\right.$$

$$\left. - \sin\left[2 \cos^{-1}\left(\frac{r_b - y}{\tan 69^o6' \sqrt{2r_b y - y^2}}\right)\right]\right\} \quad \text{(see sketch 5)}$$

$$V_{c,3} = 0$$

and

$$A_{f,3} = 0$$

These equations are valid for strokes within the limits of

$$0.06580 r_b = y_I \leqq y \leqq y_{II} = 0.20541 r_b$$

The equations for regime III are

$$V_{c,1} = V_{1,i} - \left[\frac{1}{3} A_{f,1}(r_b - y) - \frac{\pi r_p^3}{15}\right]$$

$$A_{f,1} = 0.47870 r_b^2 \left(\frac{r_b - y}{r_b \cos 37^o23'}\right)^2$$

$$V_{c,2} = \frac{\pi}{3} y^2(3r_b - y) - V_{c,1} - V_{c,3}$$

$$A_{f,2} = \pi\left(2r_b y - y^2\right) - A_{f,1} - A_{f,3}$$

$$V_{c,3} = \sum_{y_{II}}^{y} A_{f,3}\,\Delta y$$

and

$$A_{f,3} = 3\left[\frac{cL}{2} + \frac{r_f^2}{2}\left(\frac{\pi\phi}{180^o} - \sin\phi\right)\right] \qquad \text{(see sketch 5)}$$

where

$$\frac{c}{2} = r_f \sin\frac{\phi}{2}$$

$$L = \frac{c}{2\tan\frac{\alpha}{2}}$$

$$r_f = \sqrt{2r_b y - y^2}$$

and

$$\phi = 2\left\{\frac{\alpha}{2} - \sin^{-1}\left[\frac{(r_b - y)\tan 37^o23'\sin\frac{\alpha}{2}}{r_f}\right]\right\}$$

For this configuration and impact point, $\frac{\alpha}{2} = \tan^{-1}(\tan 72^o \sin 52^o37') = 67^o46'$.

The equations for regime III are applicable for values of stroke of

$$0.20541r_b = y_{II} \leqq y \leqq r_b - r_p$$

The footprint planes and elevation view for an impact at the center of the face of one compartment are shown in sketch 5.

APPENDIX B

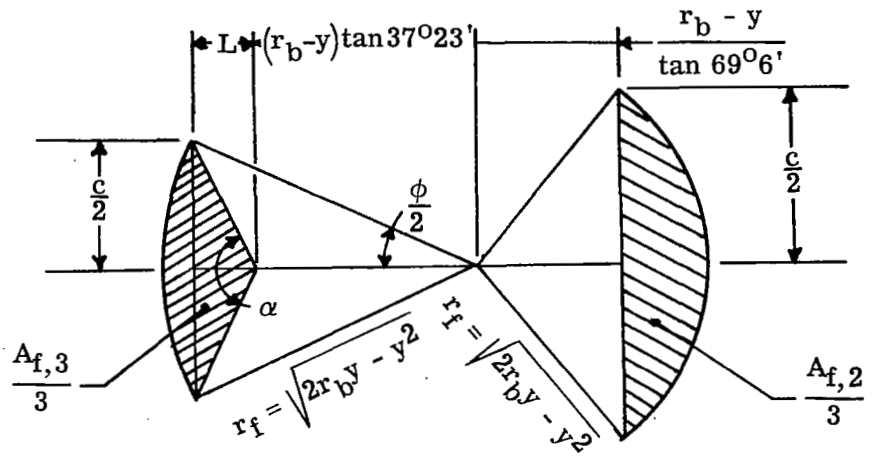

Footprint planes

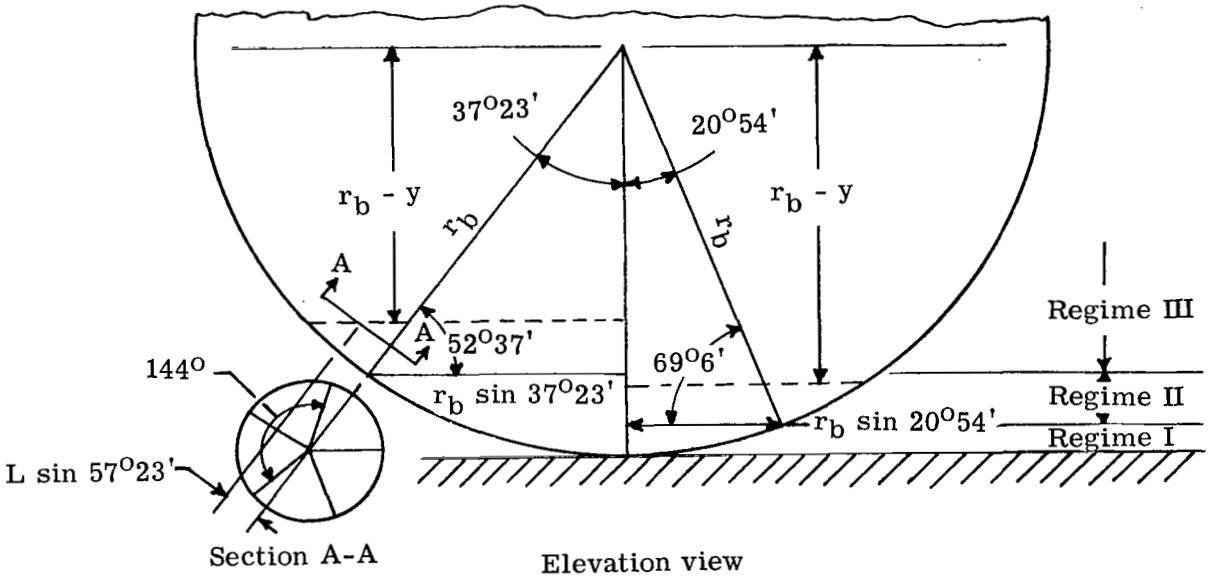

Elevation view

Sketch 5

APPENDIX C

IMPACT EQUATIONS

For an impact at a juncture of five compartments or at the center of the face of one compartment, the decelerating force at any time after impact is computed from

$$F_t = \left(P_{1,t} - P_a\right)\left(A_{f,1}\right)_t + \left(P_{2,t} - P_a\right)\left(A_{f,2}\right)_t + \left(P_{3,t} - P_a\right)\left(A_{f,3}\right)_t$$

The deceleration at any time after impact is obtained from

$$\ddot{y}_t = \frac{-F_t}{m_v} + \ddot{y}_g$$

The velocity is determined from

$$\dot{y}_t = \dot{y}_{t-1} + \ddot{y}_{t-1}\,\Delta t$$

For the next computing interval the stroke is then obtained from

$$y_t = \dot{y}_t\,\Delta t + 0.5\ddot{y}_{t-1}(\Delta t)^2$$

Impact at a Juncture of Five Compartments

The equations for the computation of an impact on the spherical bag at a juncture of five compartments are presented. The three regimes of stroke y_t that must be considered are

Regime I: $0 \leqq y_t \leqq r_b - r_b \cos 58^\circ 17'$, with only the five compartments of volume 1 involved in compression

Regime II: $r_b - r_b \cos 58^\circ 17' \leqq y_t \leqq r_b - r_b \cos 63^\circ 26'$, with the five compartments of volume 1 and the five compartments of volume 2 involved in compression

Regime III: $r_b - r_b \cos 63^\circ 26' \leqq y_t \leqq r_b - r_p$, with the five compartments each of volumes 1, 2, and 3 involved in compression

The equations involved for volumes 1, 2, 3, and 4 in regimes I, II, and III are

Regime I, volume 1:

$$V_{1,t} = V_{1,i} - \left(V_{c,1}\right)_t \tag{C1}$$

$$V_{1,i} = \frac{\pi}{3}\left(r_b^3 - r_p^3\right) \tag{C2}$$

$$\left(V_{c,1}\right)_t = \frac{\pi}{3} y_t^2 \left(3r_b - y_t\right) \tag{C3}$$

$$\left(A_{f,1}\right)_t = \pi\left(2r_b y_t - y_t^2\right) \tag{C4}$$

$$P_{1,t} = \frac{P_{1,i} V_{1,i}^{\,k}}{V_{1,t}^{\,k}} \left[\frac{m_{1,i} - \left(m_{1,e}\right)_t}{m_{1,i}}\right]^k = P_{1,i}\left(\frac{\rho_{1,t}}{\rho_{1,i}}\right)^k \tag{C5}$$

$$\left(m_{1,e}\right)_t = \sum_0^t Q_{1,t}\, \Delta t \tag{C6}$$

$$\left.\begin{aligned} Q_{1,t} &= 0.465 B_1 A_{o,1} \sqrt{\frac{Rp\rho}{H}\left(1 - \frac{P^2}{p^2}\right)} && \left(\frac{P}{p} \geqq 0.53\right) \\ Q_{1,t} &= \left(0.449 + 0.241\,\frac{P}{p}\right) B_1 A_{o,1} \sqrt{\frac{Rp\rho}{H}\left(1 - \frac{P}{p}\right)} && \left(\frac{P}{p} < 0.53\right) \end{aligned}\right\} \tag{C7}$$

(If $B_1 = \dfrac{P_{1,t-1} - P_{2,t-1}}{\left|P_{1,t-1} - P_{2,t-1}\right|} = +1$ (with only the first term of the Taylor's series expansions retained), then $\rho = \rho_{1,t-1} = \dfrac{m_{1,t-1}}{V_{1,t-1}}$, $p = P_{1,t-1}$, and $P = P_{2,t-1}$; if $B_1 = -1$, then $\rho = \rho_{2,t-1} = \dfrac{m_{2,t-1}}{V_{2,t-1}}$, $p = P_{2,t-1}$, and $P = P_{1,t-1}$.)

Regime I, volume 2:

$$V_{2,i} = \frac{\pi}{3}\left(r_b^3 - r_p^3\right) \tag{C8}$$

$$\left(A_{f,2}\right)_t = 0 \tag{C9}$$

$$P_{2,t} = \left[\frac{m_{2,i} + (m_{1,e})_t - (m_{2,e})_t}{m_{2,i}}\right]^k P_{2,i} = P_{2,i}\left(\frac{\rho_{2,t}}{\rho_{2,i}}\right)^k \tag{C10}$$

$(m_{1,e})_t$ as defined in equation (C6)

$$(m_{2,e})_t = \sum_0^t Q_{2,t}\,\Delta t \tag{C11}$$

$$\left.\begin{aligned} Q_{2,t} &= 0.465 B_2 A_{o,2}\sqrt{\frac{Rp\rho}{H}\left(1 - \frac{p^2}{p^2}\right)} && \left(\frac{P}{p} \geqq 0.53\right) \\ Q_{2,t} &= \left(0.449 + 0.241\,\frac{P}{p}\right) B_2 A_{o,2}\sqrt{\frac{Rp\rho}{H}\left(1 - \frac{P}{p}\right)} && \left(\frac{P}{p} < 0.53\right) \end{aligned}\right\} \tag{C12}$$

$$\left(\text{If } B_2 = \frac{P_{2,t-1} - P_{3,t-1}}{|P_{2,t-1} - P_{3,t-1}|} = +1, \text{ then } \rho = \rho_{2,t-1} = \frac{m_{2,t-1}}{V_{2,t-1}},\ p = P_{2,t-1}, \text{ and } P = P_{3,t-1}; \text{ if } B_2 = -1, \text{ then } \rho = \rho_{3,t-1} = \frac{m_{3,t-1}}{V_{3,t-1}},\ p = P_{3,t-1}, \text{ and } P = P_{2,t-1}.\right)$$

Regime I, volume 3:

$$V_{3,i} = \frac{\pi}{3}\left(r_b^3 - r_p^3\right) \tag{C13}$$

$$(A_{f,3})_t = 0 \tag{C14}$$

$$P_{3,t} = \left[\frac{m_{3,i} + (m_{2,e})_t - (m_{3,e})_t}{m_{3,i}}\right]^k P_{3,i} = P_{3,i}\left(\frac{\rho_{3,t}}{\rho_{3,i}}\right)^k \tag{C15}$$

$(m_{2,e})_t$ as defined in equation (C11)

$$(m_{3,e})_t = \sum_0^t Q_{3,t}\,\Delta t \tag{C16}$$

$$\left.\begin{aligned} Q_{3,t} &= 0.465 B_3 A_{o,3}\sqrt{\frac{Rp\rho}{H}\left(1 - \frac{P^2}{p^2}\right)} && \left(\frac{P}{p} \geqq 0.53\right) \\ Q_{3,t} &= \left(0.449 + 0.241\,\frac{P}{p}\right) B_3 A_{o,3}\sqrt{\frac{Rp\rho}{H}\left(1 - \frac{P}{p}\right)} && \left(\frac{P}{p} < 0.53\right) \end{aligned}\right\} \tag{C17}$$

$$\left(\text{If } B_3 = \frac{P_{3,t-1} - P_{4,t-1}}{\left|P_{3,t-1} - P_{4,t-1}\right|} = +1, \text{ then } \rho = \rho_{3,t-1} = \frac{m_{3,t-1}}{V_{3,t-1}},\ p = P_{3,t-1}, \text{ and } P = P_{4,t-1}; \text{ if } B_3 = -1, \text{ then } \rho = \rho_{4,t-1} = \frac{m_{4,t-1}}{V_{4,t-1}},\ p = P_{4,t-1}, \text{ and } P = P_{3,t-1}.\right)$$

Regime I, volume 4:

$$(A_{f,4})_t = 0 \tag{C18}$$

$$P_{4,t} = \left[\frac{m_{4,i} + (m_{3,e})_t}{m_{4,i}}\right]^k P_{4,i} = \left(\frac{\rho_{4,t}}{\rho_{4,i}}\right)^k P_{4,i} \tag{C19}$$

$(m_{3,e})_t$ as defined in equation (C16)

Regime II, volume 1:

$V_{1,t}$ as defined in equation (C1)

$V_{1,i}$ as defined in equation (C2)

$$(V_{c,1})_t = \frac{\pi}{3} y_t^2(3r_b - y_t) - (V_{c,2})_t \tag{C20}$$

$$(A_{f,1})_t = \pi(2r_b y_t - y_t^2) - (A_{f,2})_t \tag{C21}$$

$$(A_{f,2})_t = \frac{5}{2}(2r_b y_t - y_t^2)\left(\frac{2\pi}{180^o}\cos^{-1}\left[\frac{(r_b - y_t)\tan 58^o17'}{\sqrt{2r_b y_t - y_t^2}}\right]\right.$$

$$\left. - \sin\left\{2\cos^{-1}\left[\frac{(r_b - y_t)\tan 58^o17'}{\sqrt{2r_b y_t - y_t^2}}\right]\right\}\right) \tag{C22}$$

$P_{1,t}$ as defined in equation (C5)

$(m_{1,e})_t$ as defined in equation (C6)

Regime II, volume 2:

$$V_{2,t} = V_{2,i} - (V_{c,2})_t \tag{C23}$$

$V_{2,i}$ as defined in equation (C8)

$$(V_{c,2})_t = \sum_{y_I}^{y} (A_{f,2})_t \, \Delta y \tag{C24}$$

$(A_{f,2})_t$ as defined in equation (C22)

$$P_{2,t} = \frac{P_{2,i}V_{2,i}^k}{V_{2,t}^k}\left[\frac{m_{2,i} + (m_{1,e})_t - (m_{2,e})_t}{m_{2,i}}\right]^k = P_{2,i}\left(\frac{\rho_{2,t}}{\rho_{2,i}}\right)^k \tag{C25}$$

$(m_{2,e})_t$ as defined in equation (C11)

APPENDIX C

Regime II, volume 3:

$(A_{f,3})_t$ as defined in equation (C14)

$P_{3,t}$ as defined in equation (C15)

$(m_{2,e})_t$ as defined in equation (C11)

$(m_{3,e})_t$ as defined in equation (C16)

Regime II, volume 4:

$(A_{f,4})_t$ as defined in equation (C18)

$P_{4,t}$ as defined in equation (C19)

$(m_{3,e})_t$ as defined in equation (C16)

Regime III, volume 1:

$V_{1,i}$ as defined in equation (C2)

$$V_{1,t} = \frac{5}{6} \sin 72^{\circ} \tan^2 63^{\circ}26' (r_b - y_t)^3 - \frac{\pi r_p^3}{3} \tag{C26}$$

$$(A_{f,1})_t = \frac{5}{2} \sin 72^{\circ} \tan^2 63^{\circ}26' (r_b - y_t)^2 \tag{C27}$$

$P_{1,t}$ as defined in equation (C5)

$(m_{1,e})_t$ as defined in equation (C6)

Regime III, volume 2:

$V_{2,t}$ as defined in equation (C23)

$$(V_{c,2})_t = \frac{\pi}{3} y_t^2 (3r_b - y_t) - (V_{c,1})_t - (V_{c,3})_t \tag{C28}$$

$$(V_{c,1})_t = V_{1,i} - V_{1,t} \tag{C29}$$

$V_{1,t}$ as defined in equation (C26)

$$\left(V_{c,3}\right)_t = \sum_{y_{II}}^{y} \left(A_{f,3}\right)_t \Delta y \tag{C30}$$

$$\left(A_{f,3}\right)_t = 5\left[\frac{cL}{2} + \frac{r_f^2}{2}\left(\frac{\pi\phi}{180^o} - \sin\phi\right)\right] \tag{C31}$$

$$\left(\text{In equation (C31): } \frac{c}{2} = r_f \sin\frac{\phi}{2}, \quad L = \frac{c}{2\tan\frac{\alpha}{2}}, \quad r_f = \sqrt{2r_b y_t - y_t^2}, \text{ and } \phi = \alpha - 2\sin^{-1}\left[\frac{(r_b - y_t)\tan 63^o26' \sin\frac{\alpha}{2}}{r_f}\right], \text{ with } \alpha = 36^o.\right)$$

$$\left(A_{f,2}\right)_t = \pi\left(2r_b y_t - y_t^2\right) - \left(A_{f,1}\right)_t - \left(A_{f,3}\right)_t \tag{C32}$$

$\left(A_{f,1}\right)_t$ as defined in equation (C27)

$\left(A_{f,3}\right)_t$ as defined in equation (C31)

$P_{2,t}$ as defined in equation (C25)

$\left(m_{1,e}\right)_t$ as defined in equation (C6)

$\left(m_{2,e}\right)_t$ as defined in equation (C11)

Regime III, volume 3:

$$V_{3,t} = V_{3,i} - \left(V_{c,3}\right)_t \tag{C33}$$

$\left(V_{c,3}\right)_t$ as defined in equation (C30)

$\left(A_{f,3}\right)_t$ as defined in equation (C31)

$$P_{3,t} = \frac{P_{3,i}V_{3,i}^{k}}{V_{3,t}^{k}}\left[\frac{m_{3,i} + (m_{2,e})_t - (m_{3,e})_t}{m_{3,i}}\right]^k = P_{3,i}\left(\frac{\rho_{3,t}}{\rho_{3,i}}\right)^k \quad \text{(C34)}$$

$(m_{2,e})_t$ as defined in equation (C11)

$(m_{3,e})_t$ as defined in equation (C16)

Regime III, volume 4:

$(A_{f,4})_t$ as defined in equation (C18)

$P_{4,t}$ as defined in equation (C19)

$(m_{3,e})_t$ as defined in equation (C16)

Impact at the Center of the Face of One Compartment

The equations for the computation of the deceleration characteristics for impact on the surface of the sphere at the center of the face of one compartment are presented. The three regimes of stroke y_t that must be considered are

Regime I: $0 \leqq y_t \leqq 0.06580r_b$, with the one compartment of volume 1 involved in the compression

Regime II: $0.06580r_b \leqq y_t \leqq 0.20541r_b$, with the one compartment of volume 1 and the three compartments of volume 2 involved in the compression

Regime III: $0.20541r_b \leqq y_t \leqq r_b - r_p$, with the one compartment of volume 1, the three compartments of volume 2, and the six compartments of volume 3 involved in the compressions

The equations involved for volumes 1, 2, 3, 4, 5, and 6 in regimes I, II, and III are

Regime I, volume 1:

$V_{1,t}$ as defined in equation (C1)

$$V_{1,i} = \frac{\pi}{15}(r_b^3 - r_p^3) \quad \text{(C35)}$$

$(V_{c,1})_t$ as defined in equation (C3)

$(A_{f,1})_t$ as defined in equation (C4)

$P_{1,t}$ as defined in equation (C5)

$(m_{1,e})_t$ as defined in equation (C6)

$Q_{1,t}$ as defined in equations (C7)

Regime I, volume 2:

$$V_{2,i} = \frac{\pi}{5}\left(r_b^3 - r_p^3\right) \tag{C36}$$

$(A_{f,2})_t$ as defined in equation (C9)

$P_{2,t}$ as defined in equation (C10)

$(m_{1,e})_t$ as defined in equation (C6)

$(m_{2,e})_t$ as defined in equation (C11)

$Q_{2,t}$ as defined in equations (C12)

Regime I, volume 3:

$$V_{3,i} = \frac{2\pi}{5}\left(r_b^3 - r_p^3\right) \tag{C37}$$

$(A_{f,3})_t$ as defined in equation (C14)

$P_{3,t}$ as defined in equation (C15)

$(m_{2,e})_t$ as defined in equation (C11)

$(m_{3,e})_t$ as defined in equation (C16)

$Q_{3,t}$ as defined in equations (C17)

Regime I, volume 4:

$$V_{4,i} = V_{3,i} \tag{C38}$$

$(A_{f,4})_t$ as defined in equation (C18)

$$P_{4,t} = \left[\frac{m_{4,i} + (m_{3,e})_t - (m_{4,e})_t}{m_{4,i}}\right]^k P_{4,i} = P_{4,i}\left(\frac{\rho_{4,t}}{\rho_{4,i}}\right)^k \tag{C39}$$

$(m_{3,e})_t$ as defined in equation (C16)

$$(m_{4,e})_t = \sum_0^t Q_{4,t}\,\Delta t \tag{C40}$$

$$\left.\begin{aligned} Q_{4,t} &= 0.465 B_4 A_{o,4}\sqrt{\frac{Rp\rho}{H}\left(1 - \frac{P^2}{p^2}\right)} && \left(\frac{P}{p} \geqq 0.53\right) \\ Q_{4,t} &= \left(0.449 + 0.241\,\frac{P}{p}\right) B_4 A_{o,4}\sqrt{\frac{Rp\rho}{H}\left(1 - \frac{P}{p}\right)} && \left(\frac{P}{p} < 0.53\right) \end{aligned}\right\} \tag{C41}$$

$$\left(\text{If } B_4 = \frac{P_{4,t-1} - P_{5,t-1}}{|P_{4,t-1} - P_{5,t-1}|} = +1, \text{ then } \rho = \rho_{4,t-1} = \frac{m_{4,t-1}}{V_{4,t-1}},\ p = P_{4,t-1}, \text{ and } P = P_{5,t-1}; \text{ if } B_4 = -1, \text{ then } \rho = \rho_{5,t-1} = \frac{m_{5,t-1}}{V_{5,t-1}},\ p = P_{5,t-1}, \text{ and } P = P_{4,t-1}.\right)$$

Regime I, volume 5:

$$V_{5,i} = V_{2,i} \tag{C42}$$

$$(A_{f,5})_t = 0 \tag{C43}$$

$$P_{5,t} = \left[\frac{m_{5,i} + (m_{4,e})_t - (m_{5,e})_t}{m_{5,i}}\right]^k P_{5,i} = P_{5,i}\left(\frac{\rho_{5,t}}{\rho_{5,i}}\right)^k \tag{C44}$$

$(m_{4,e})_t$ as defined in equation (C40)

$$(m_{5,e})_t = \sum_{0}^{t} Q_{5,t}\,\Delta t \tag{C45}$$

$$\left.\begin{aligned} Q_{5,t} &= 0.465 B_5 A_{o,5}\sqrt{\frac{Rp\rho}{H}\left(1 - \frac{P^2}{p^2}\right)} && \left(\frac{P}{p} \geqq 0.53\right) \\ Q_{5,t} &= \left(0.449 + 0.241\,\frac{P}{p}\right) B_5 A_{o,5}\sqrt{\frac{Rp\rho}{H}\left(1 - \frac{P}{p}\right)} && \left(\frac{P}{p} < 0.53\right) \end{aligned}\right\} \tag{C46}$$

$$\left(\text{If } B_5 = \frac{P_{5,t-1} - P_{6,t-1}}{|P_{5,t-1} - P_{1,t-1}|} = +1, \text{ then } \rho = \rho_{5,t-1} = \frac{m_{5,t-1}}{V_{5,t-1}},\ p = P_{5,t-1}, \text{ and } P = P_{6,t-1}; \text{ if } B_5 = -1, \text{ then } \rho = \rho_{6,t-1} = \frac{m_{6,t-1}}{V_{6,t-1}},\ p = P_{6,t-1}, \text{ and } P = P_{5,t-1}.\right)$$

Regime I, volume 6:

$$V_{6,i} = V_{1,i} \tag{C47}$$

$$(A_{f,6})_t = 0 \tag{C48}$$

$$P_{6,t} = \left[\frac{m_{6,i} + (m_{5,e})_t}{m_{6,i}}\right]^k P_{6,i} = P_{6,i}\left(\frac{\rho_{6,t}}{\rho_{6,i}}\right)^k \tag{C49}$$

$(m_{5,e})_t$ as defined in equation (C45)

Regime II, volume 1:

$V_{1,t}$ as defined in equation (C1)

$V_{1,i}$ as defined in equation (C35)

$(V_{c,1})_t$ as defined in equation (C20)

$$(V_{c,2})_t = \sum_{0}^{t} (A_{f,2})_t \, \Delta t \tag{C50}$$

$(A_{f,1})_t$ as defined in equation (C21)

$$(A_{f,2})_t = \frac{3}{2}\left(2r_b y_t - y_t^2\right)\left(\frac{2\pi}{180^o} \cos^{-1}\left[\frac{(r_b - y_t)\tan 20^o54'}{\sqrt{2r_b y_t - y_t^2}}\right]\right.$$

$$\left. - \sin\left\{2 \cos^{-1}\left[\frac{(r_b - y_t)\tan 20^o54'}{\sqrt{2r_b y_t - y_t^2}}\right]\right\}\right) \tag{C51}$$

$P_{1,t}$ as defined in equation (C5)

$(m_{1,e})_t$ as defined in equation (C6)

Regime II, volume 2:

$V_{2,t}$ as defined in equation (C23)

$V_{2,i}$ as defined in equation (C36)

$(V_{c,2})_t$ as defined in equation (C50)

$(A_{f,2})_t$ as defined in equation (C51)

$P_{2,t}$ as defined in equation (C25)

$(m_{1,e})_t$ as defined in equation (C6)

$(m_{2,e})_t$ as defined in equation (C11)

Regime II, volume 3:

$(A_{f,3})_t$ as defined in equation (C14)

$P_{3,t}$ as defined in equation (C15)

Regime II, volume 4:

$(A_{f,4})_t$ as defined in equation (C18)

$P_{4,t}$ as defined in equation (C39)

Regime II, volume 5:

$(A_{f,5})_t$ as defined in equation (C43)

$P_{5,t}$ as defined in equation (C44)

Regime II, volume 6:

$(A_{f,6})_t$ as defined in equation (C48)

$P_{6,t}$ as defined in equation (C49)

Regime III, volume 1:

$V_{1,t}$ as defined in equation (C1)

$V_{1,i}$ as defined in equation (C35)

$$(V_{c,1})_t = \sum_{y=0}^{y_{II}} (A_{f,1})_t \, \Delta y + \sum_{y_{II}}^{y} (A_{f,1})_t \, \Delta y \tag{C52}$$

$$(A_{f,1})_t = 0.47870 r_b^2 \left(\frac{r_b - y_t}{r_b \cos 37^o 23'} \right)^2 \tag{C53}$$

$P_{1,t}$ as defined in equation (C5)

$(m_{1,e})_t$ as defined in equation (C6)

Regime III, volume 2:

$V_{2,t}$ as defined in equation (C23)

$V_{2,i}$ as defined in equation (C36)

$(V_{c,2})_t$ as defined in equation (C28)

$(V_{c,1})_t$ as defined in equation (C52)

$(V_{c,3})_t$ as defined in equation (C30)

$$(A_{f,3})_t = 3\left[\frac{cL}{2} + \frac{r_f^2}{2}\left(\frac{\pi\phi}{180^o} - \sin\phi\right)\right] \qquad \text{(C54)}$$

(In equation (C54): $\frac{c}{2} = r_f \sin\frac{\phi}{2}$, $L = \frac{c}{2}\tan\frac{\alpha}{2}$, $r_f = \sqrt{2r_b y_t - y_t^2}$, and

$\phi = 2\left\{\frac{\alpha}{2} - \sin^{-1}\left[\frac{(r_b - y_t)\tan 37^o23' \sin\frac{\alpha}{2}}{r_f}\right]\right\}$, with $\frac{\alpha}{2} = 67^o46'$.)

$(A_{f,2})_t$ as defined in equation (C32)

$(A_{f,1})_t$ as defined in equation (C53)

$(A_{f,3})_t$ as defined in equation (C54)

$P_{2,t}$ as defined in equation (C25)

$(m_{2,e})_t$ as defined in equation (C11)

Regime III, volume 3:

$V_{3,t}$ as defined in equation (C33)

$V_{3,i}$ as defined in equation (C37)

$(V_{c,3})_t$ as defined in equation (C30)

$(A_{f,3})_t$ as defined in equation (C54)

$P_{3,t}$ as defined in equation (C34)

$(m_{2,e})_t$ as defined in equation (C11)

$(m_{3,e})_t$ as defined in equation (C16)

Regime III, volume 4:

$(A_{f,4})_t$ as defined in equation (C18)

$P_{4,t}$ as defined in equation (C39)

Regime III, volume 5:

$(A_{f,5})_t$ as defined in equation (C43)

$P_{5,t}$ as defined in equation (C44)

Regime III, volume 6:

$(A_{f,6})_t$ as defined in equation (C48)

$P_{6,t}$ as defined in equation (C49)

APPENDIX D

MASS ANALYSIS OF SELECTED SPHERICAL GAS BAG

A mass analysis for the selected spherical-gas-bag landing system is presented. Maximum internal pressure and temperature result during a landing when the initial impact occurs at a juncture of five compartments. Therefore, the maximum pressure which occurs during a landing of the vehicle at a juncture of five compartments is used in the mass analysis. For a juncture impact the maximum pressure occurs in only five compartments, but since any set of five compartments may be subjected to this pressure, the maximum pressure is assumed to exist throughout the sphere.

A high-temperature nylon fabric with a neoprene coating is used in this analysis. A limited number of specimens of uncoated and coated nylon fabric were tested to determine the strength of the material. The uncoated fabric is 0.7-kg/m^2 (20-oz/yd^2) material, and tests of three specimens show that this material fails at approximately 158 kN/m (900 lbf/in.). The neoprene-coated fabric is 1.0-kg/m^2 (29-oz/yd^2) material, and tests of two specimens show that this material fails at approximately 149 kN/m (850 lbf/in.). The strength values quoted were obtained at ambient temperature and pressure. Because of the limited amount of material available for making the specimens, these strength values are approximate but are considered to be adequate for this mass analysis.

The circumferential force per unit length of a thin-walled sphere is one-half the product of bag radius and maximum gage pressure. Therefore for a maximum gage pressure of 345 kN/m^2 (50 lbf/in^2) and a bag radius of 0.9 meter (3 feet), the circumferential force in the bag envelope is 155 kN/m (900 lbf/in.). Since the coated material failed at approximately 149 kN/m (850 lbf/in.), the outer envelope is assumed to consist of two plys of the fabric in order to provide a contingency factor.

The mass of the outer-envelope material is

$$M_O = 2\left(4\pi r_b{}^2 K\right) \tag{D1}$$

where K is the mass per unit area per ply of material (that is, 1 kg/m^2 (20 oz/yd^2)). Thus $M_O = 8\pi(0.81)(1) = 20$ kilograms (1.4 slugs).

With the assumption that the compartment walls consist of one ply of fabric, the mass of material required for the 30 walls, each of which has an area of 0.467 meter^2 (5.03 feet^2) is

$$M_W = nA_W K \tag{D2}$$

where n is the number of walls and A_W is the area per wall. Thus $M_W = (30)(0.467)(1) = 14$ kilograms (1.0 slug).

With the assumption that an inner bag envelope consists of a single ply of fabric, the mass of the inner-envelope material is expressed as

$$M_I = 4\pi r_p^2 K \tag{D3}$$

Thus $M_I = 4\pi(0.09)(1) = 1$ kilogram (0.1 slug).

The total mass of bag material is

$$M_T = M_O + M_W + M_I \tag{D4}$$

which with the results from equations (D1) to (D3) yields $M_T = 35$ kilograms (2.5 slugs).

With the assumption of a seam mass of 50 percent of the total bag mass, the mass of the compartmented spherical bag is

$$M_{T'} = 1.5M_T \tag{D5}$$

which yields $M_{T'} = 53$ kilograms (3.7 slugs).

The mass of air (M_{air}) required to fill the selected bag to the specified initial pressure is 4 kilograms (0.28 slug). The mass of a pressure bottle (M_{bottle}) for storing the pressurizing air at 28 MN/m^2 (4000 lbf/in^2) is estimated to be 4 kilograms (0.3 slug), and the mass of the filling valve and manifold (M_{valve}) is estimated to be 1 kilogram (0.1 slug). The total landing-system mass is

$$m_{ls} = M_{T'} + M_{air} + M_{bottle} + M_{valve} \tag{D6}$$

Therefore, $m_{ls} = 53 + 4 + 4 + 1 = 62$ kilograms (4.3 slugs).

With the selected vehicle mass being 230 kilograms (15.735 slugs) and the estimated landing-system mass being 62 kilograms (4.3 slugs), the landing-system mass is approximately one-fourth of the vehicle mass.

REFERENCES

1. Tomcsak, Stephen L.: Decelerator Bag Study. WADC TR 59-775, U.S. Air Force, June 1960.

2. Matlock, Hudson; and Thompson, J. Neils: High-Velocity Impact Cushioning. Part III – Preliminary Tests on a Nonpressurized Air Bag. Contract DA 19-129-QM-817, Struct. Mech. Res. Lab., Univ. of Texas, Oct. 15, 1957. (Available from DDC as AD No. 220 822.)

3. Boynton, John H.: Spacecraft Systems Development and Performance. Mercury Project Summary Including Results of the Fourth Manned Orbital Flight, May 15 and 16, 1963, NASA SP-45, 1963, pp. 39-67.

4. Martin, E. Dale; and Howe, John T.: An Analysis of the Impact Motion of an Inflated Sphere Landing Vehicle. NASA TN D-314, 1960.

5. Howe, John T.; and Martin, E. Dale: Gas Dynamics of an Inflated Sphere Striking a Surface. NASA TN D-315, 1960.

6. McGehee, John R.: Investigation of a Compartmented-Gas-Bag Landing System Having Multiple-Impact Capabilities. NASA TN D-4710, 1968.

7. Comm. on Metric Pract.: ASTM Metric Practice Guide. NBS Handbook 102, U.S. Dep. Com., Mar. 10, 1967.

8. Perry, J. A., Jr.: Critical Flow Through Sharp-Edged Orifices. Trans. ASME, vol. 71, no. 7, Oct. 1949, pp. 757-764.

9. Cox, Glen N.; and Germano, F. J.: Fluid Mechanics. D. Van Nostrand Co., Inc., c.1941, p. 161.

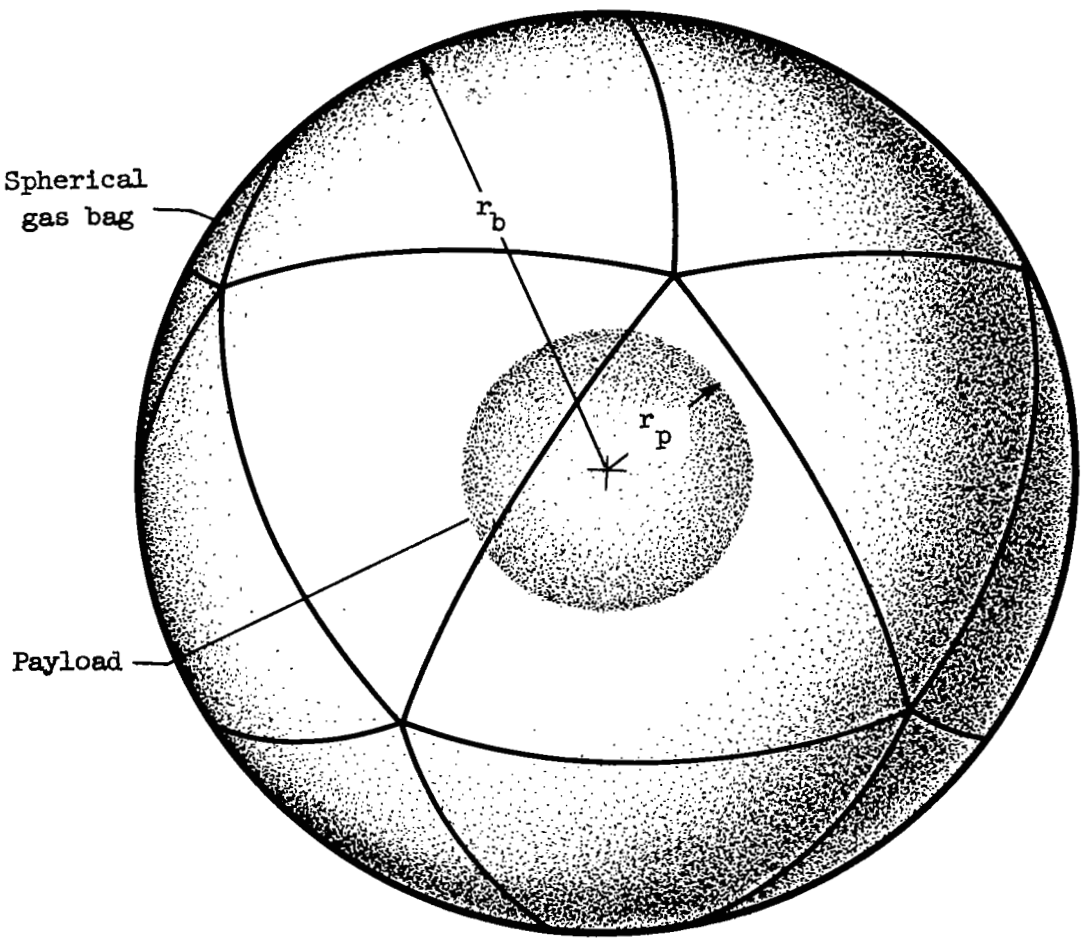

Figure 1.- Configuration of spherical-gas-bag landing system and payload.

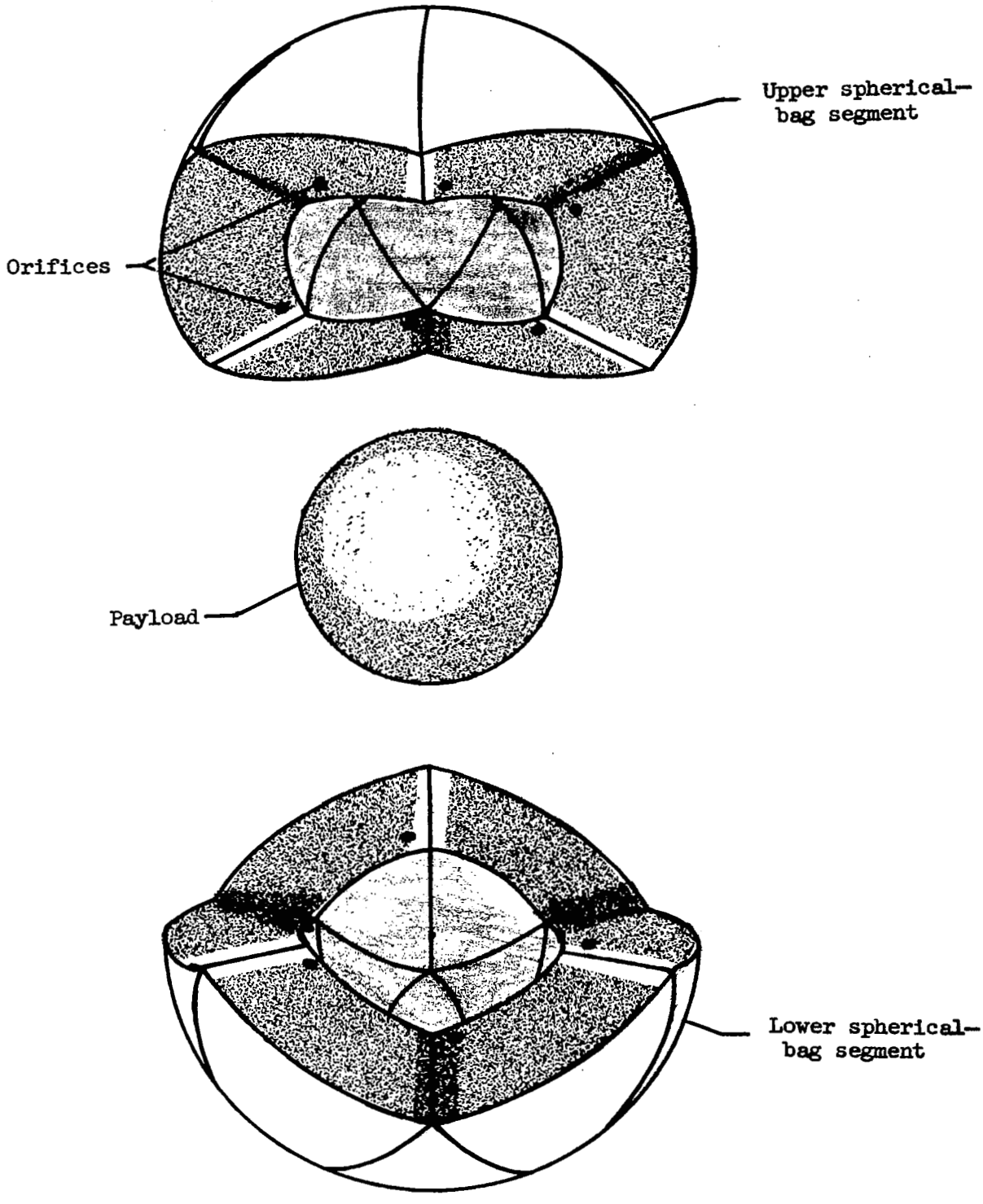

Figure 2.- Exploded view of configuration.

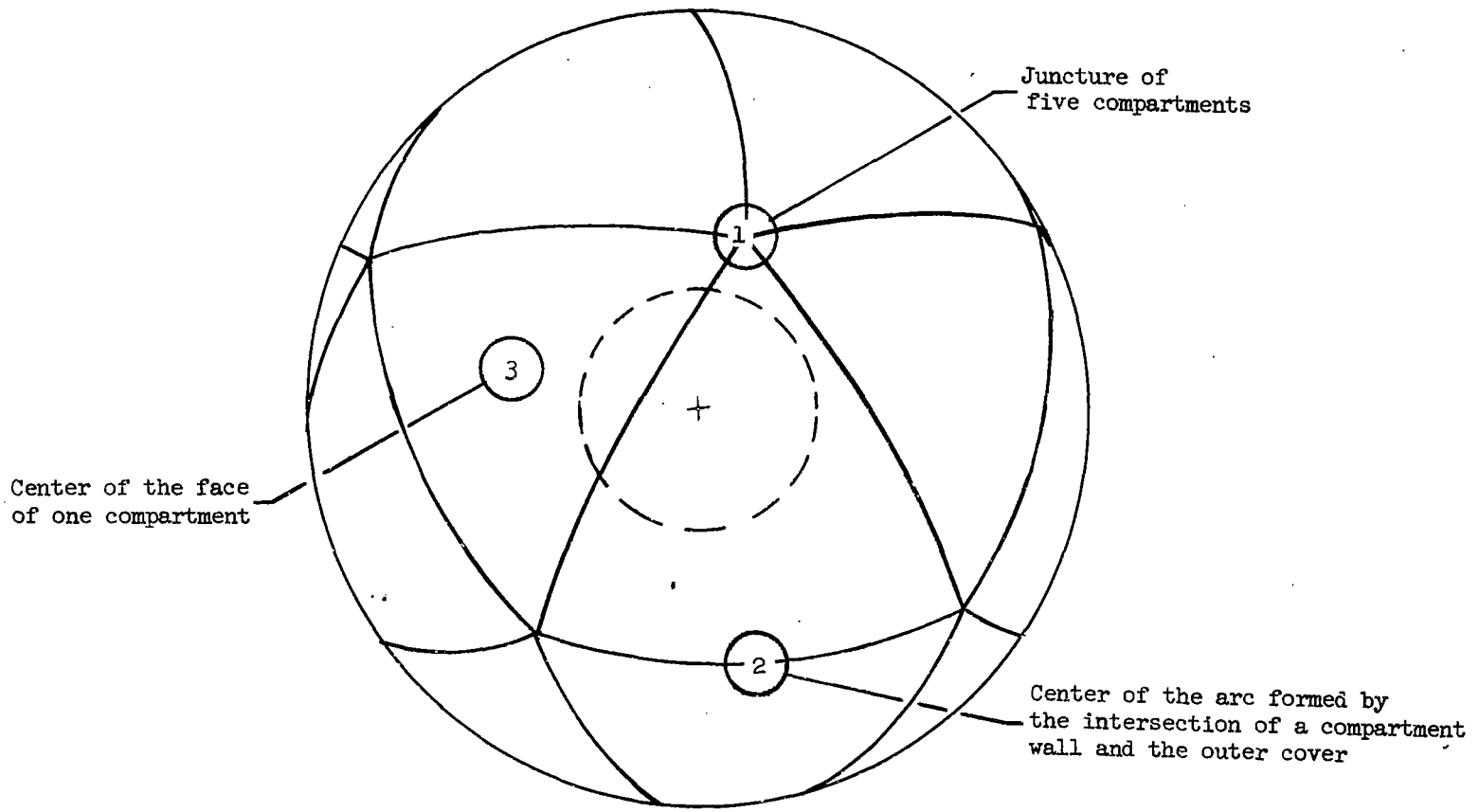

Figure 3.- Points on surface of spherical bag at which impact results in major variation of impact parameters.

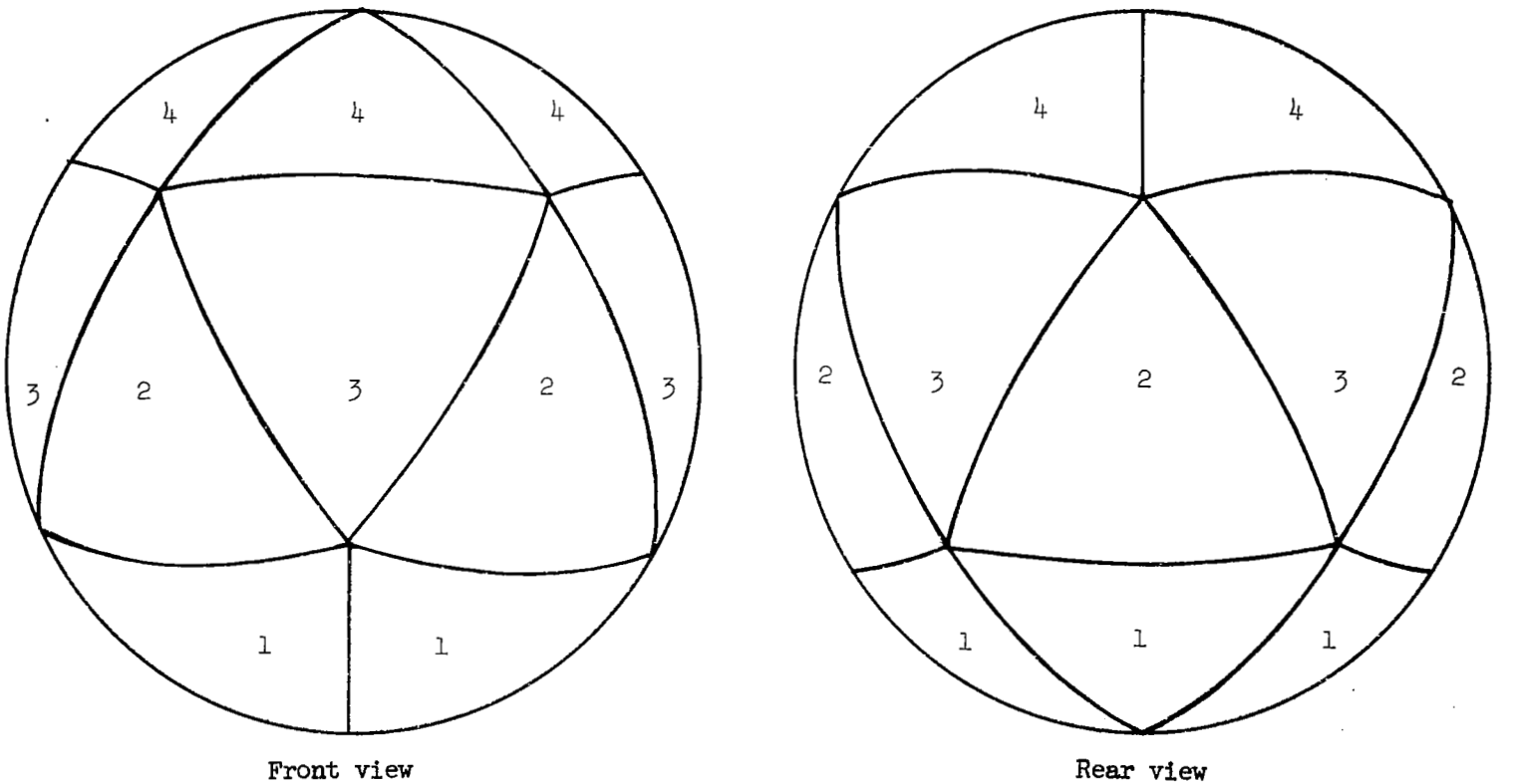

(a) Compartment symmetry. (Numbers denote compartments having the same instantaneous values of the gas parameters.)

Figure 4.- Geometry for an impact at a juncture of five compartments.

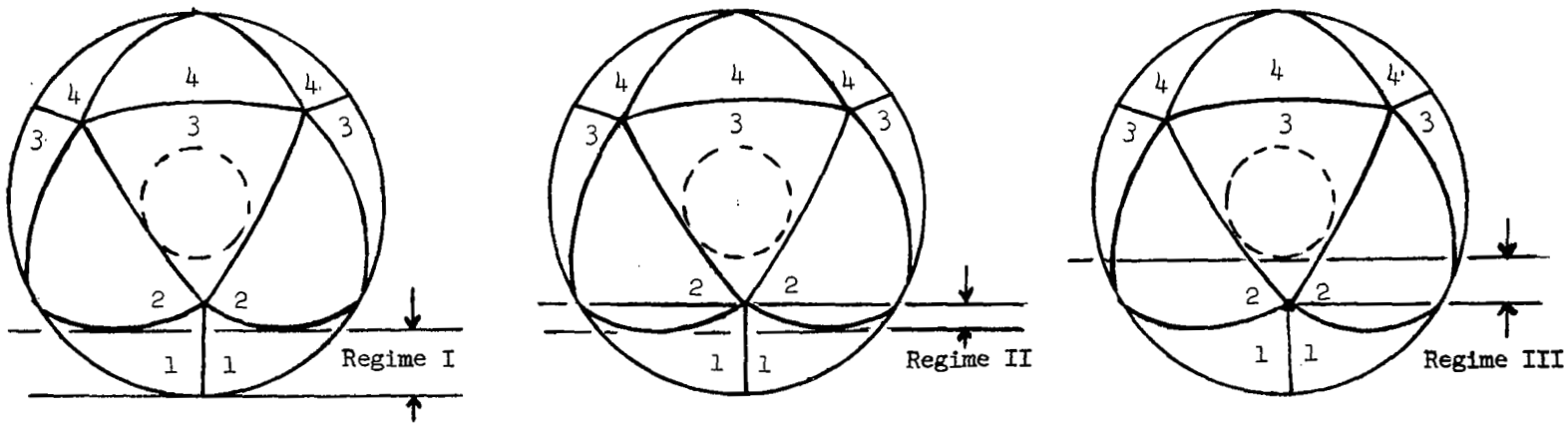

(b) Effect of stroke on compartment distortion.

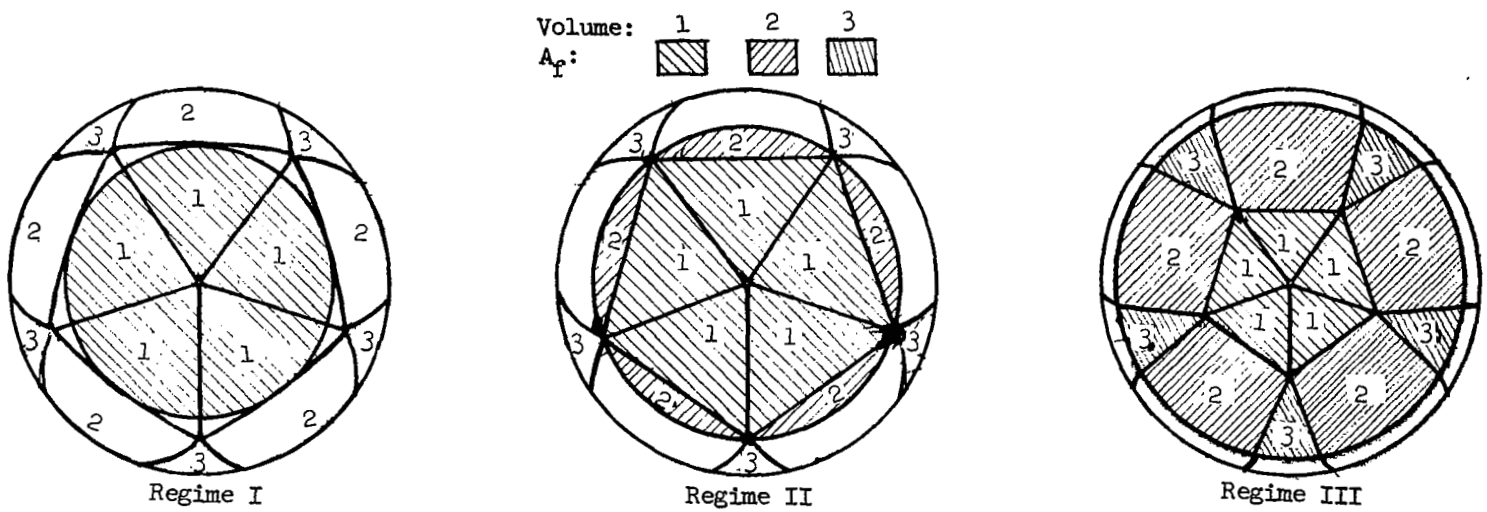

(c) Effect of stroke on footprint-area patterns.

Figure 4.- Concluded.

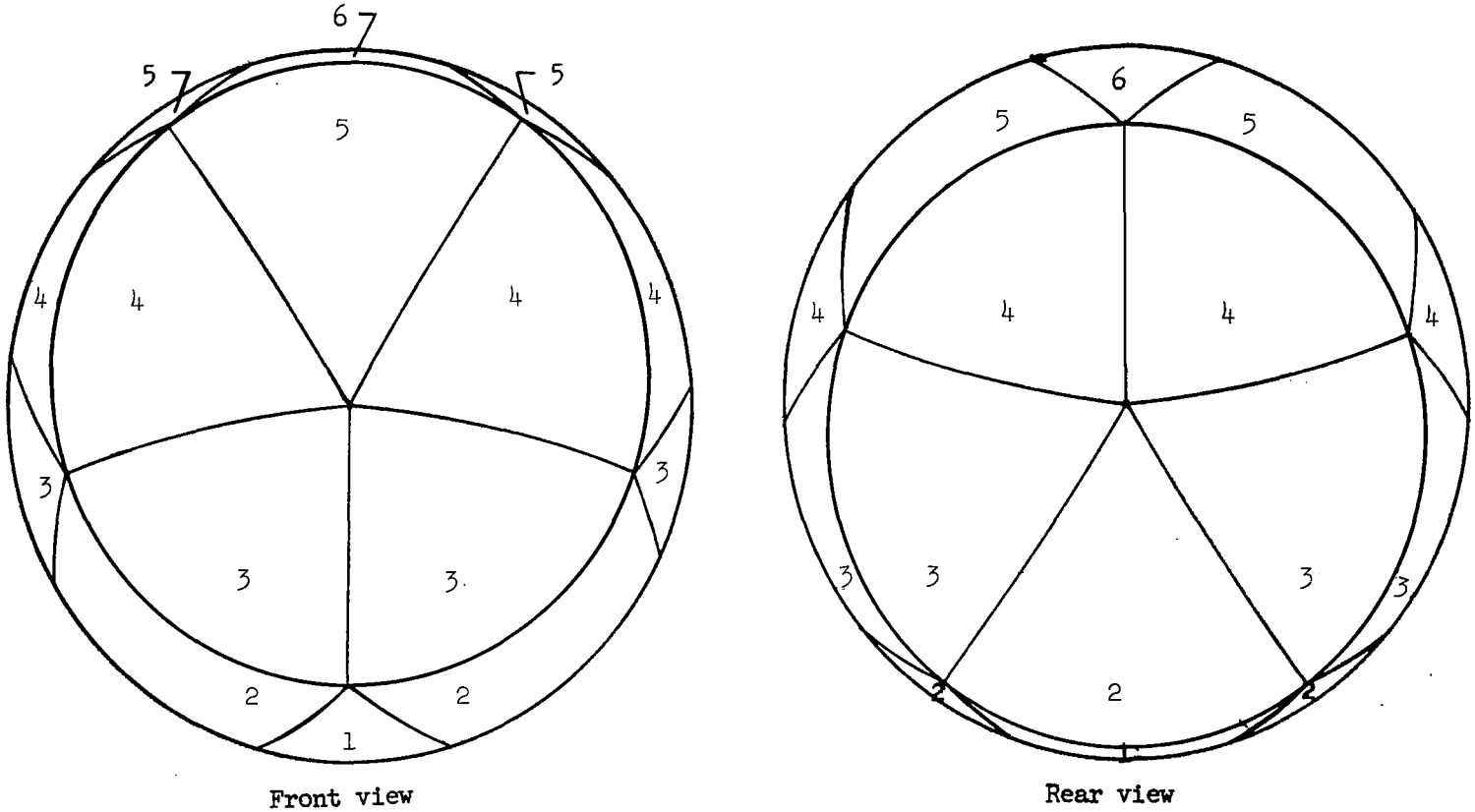

(a) Compartment symmetry. (Numbers denote compartments having the same instantaneous values of the gas parameters.)

Figure 5.- Geometry for an impact at the center of the face of one compartment.

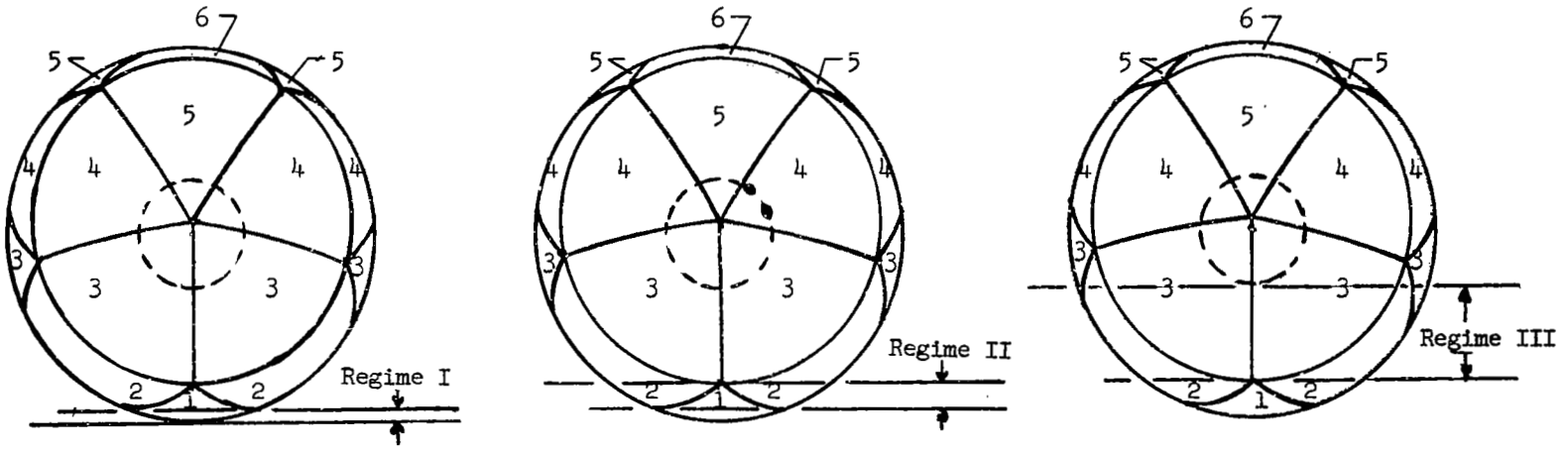

(b) Effect of stroke on compartment distortion.

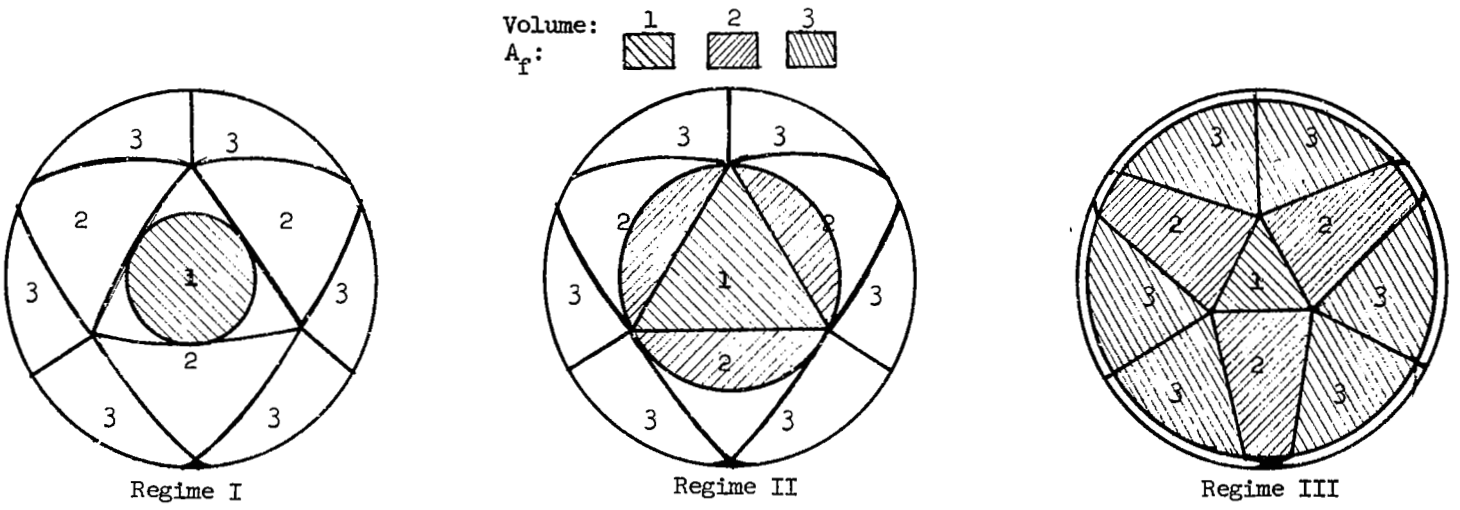

(c) Effect of stroke on footprint-area patterns.

Figure 5.- Concluded.

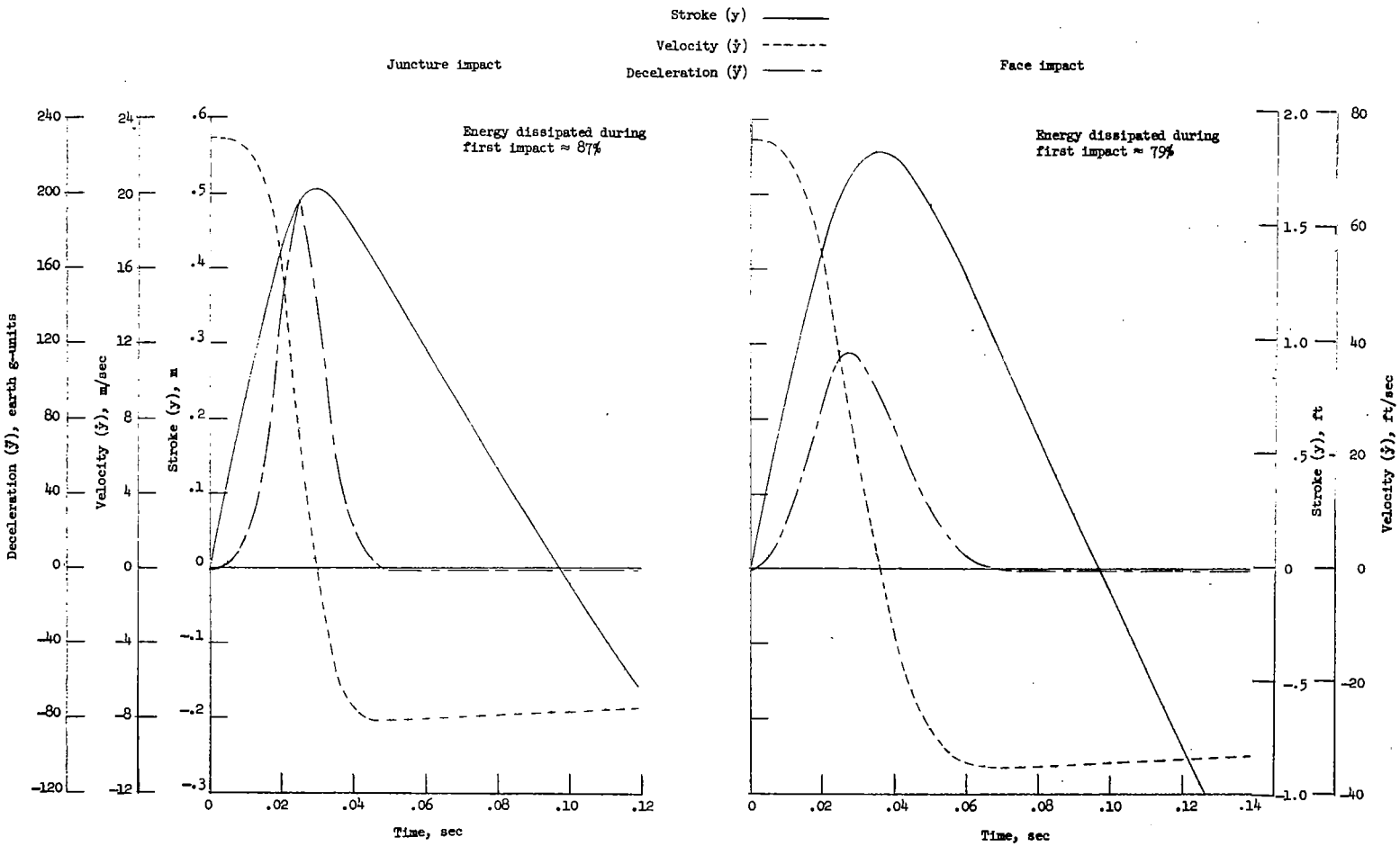

(a) Time histories of deceleration, velocity, and stroke.

Figure 6.- Time histories of deceleration, velocity, stroke, gas temperature, and compartment pressures for the critical impact points.

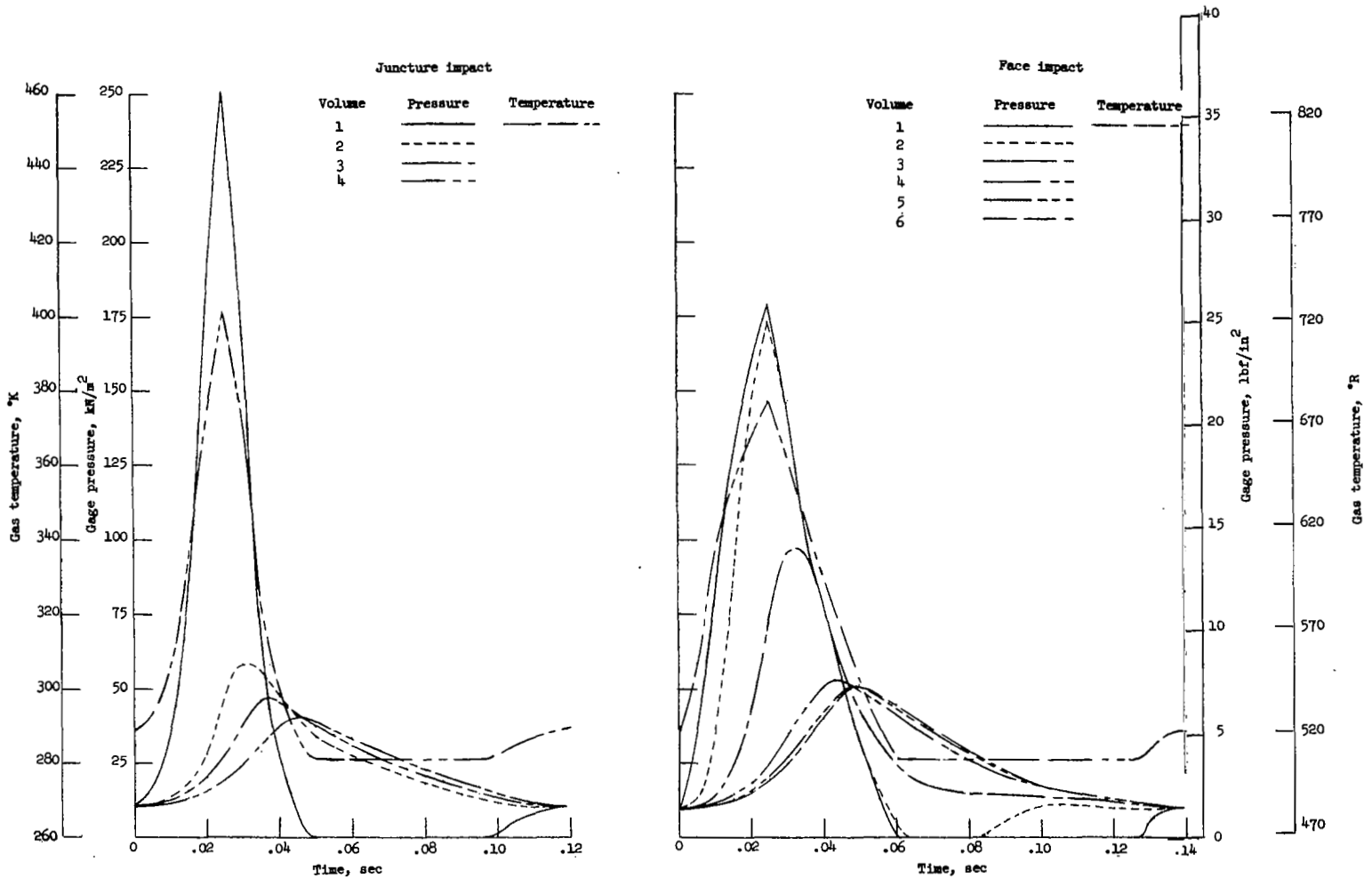

(b) Time histories of gas temperatures and pressures for the defined volumes.

Figure 6.- Concluded.

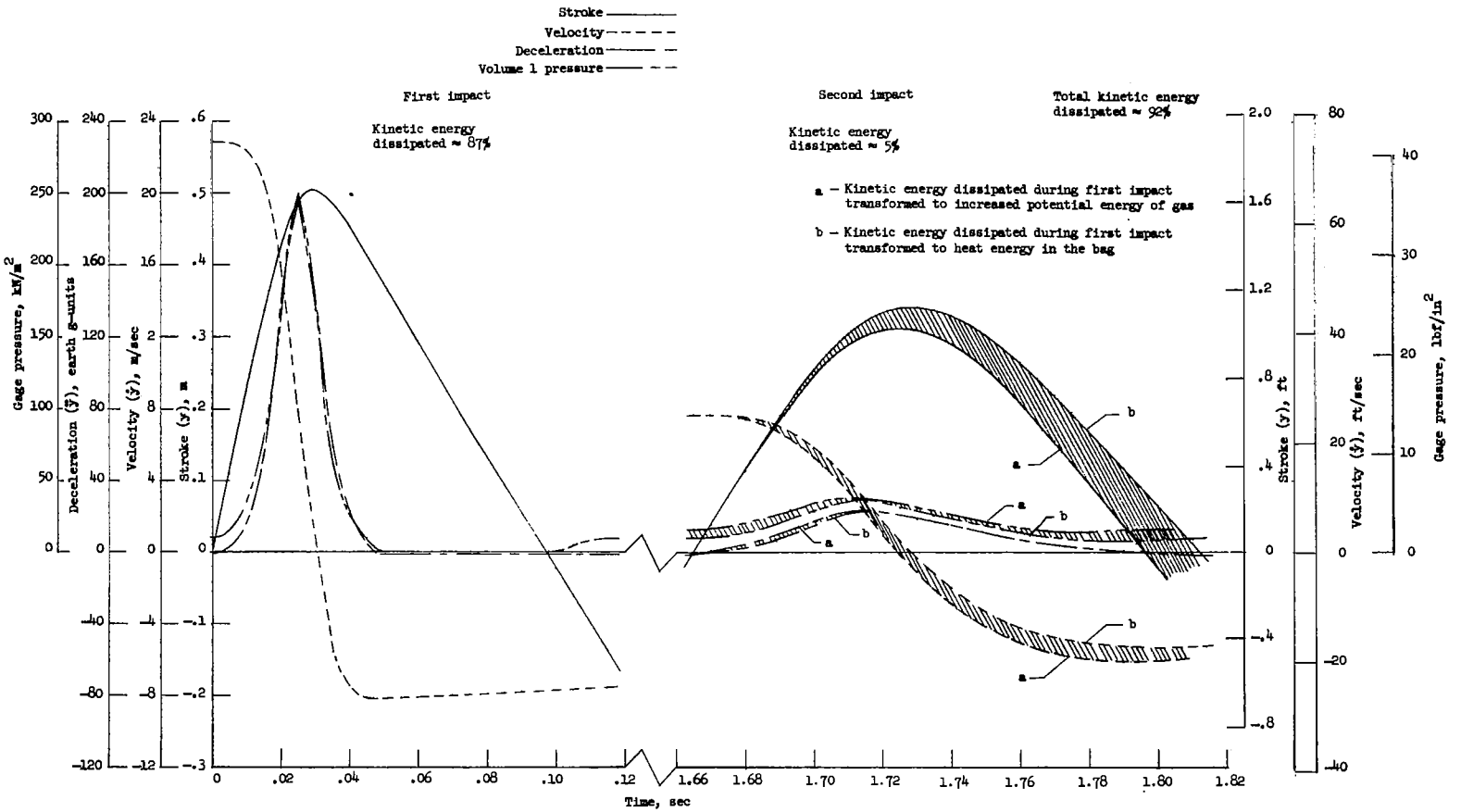

(a) Impacts at the juncture of five compartments.

Figure 7.- Time histories of deceleration, velocity, stroke, and volume 1 pressure during first and second impacts at the critical impact points.

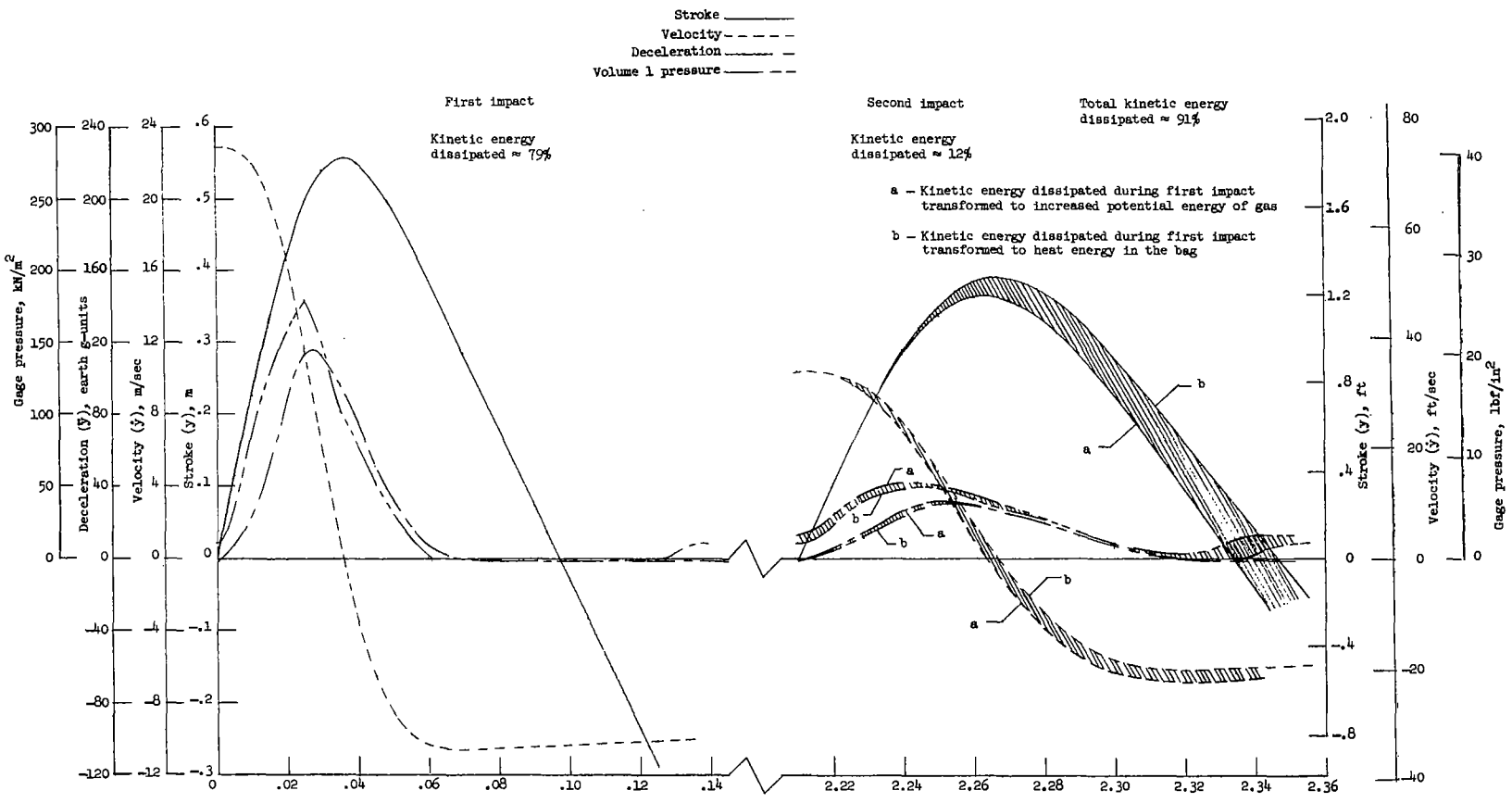

(b) Impacts at the center of the face of one compartment.

Figure 7.- Concluded.

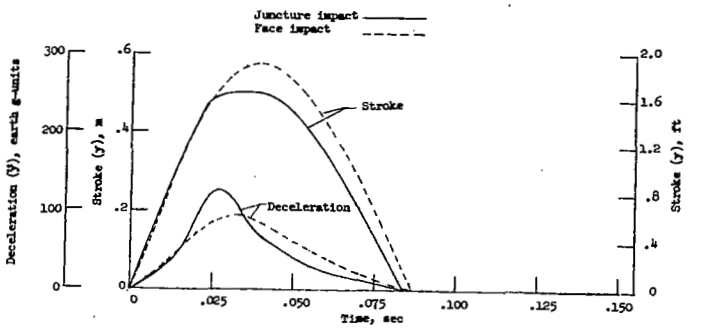

(a) Zero ambient pressure; initial bag pressure of 48 kN/m^2 (1000 lbf/ft^2).

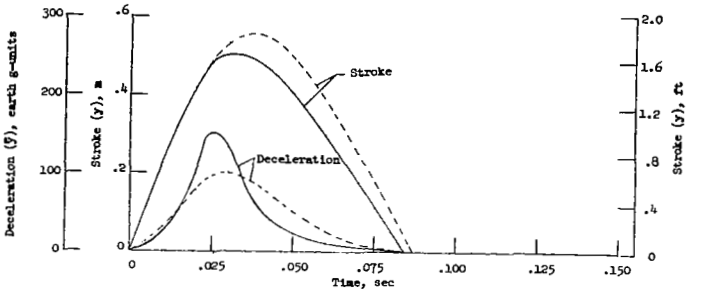

(b) Ambient pressure of 34 kN/m^2 (706 lbf/ft^2); initial bag pressure of 72 kN/m^2 (1500 lbf/ft^2).

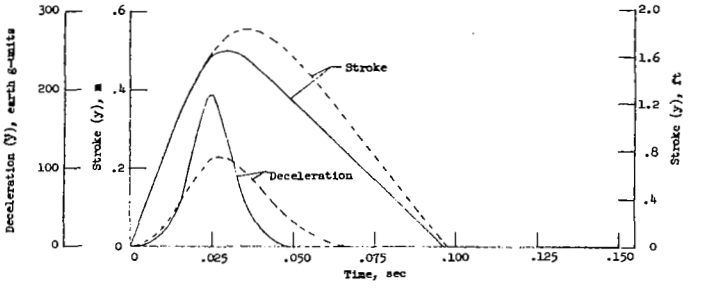

(c) Ambient pressure of 101 kN/m^2 (2117 lbf/ft^2); initial bag pressure of 111 kN/m^2 (2329 lbf/ft^2).

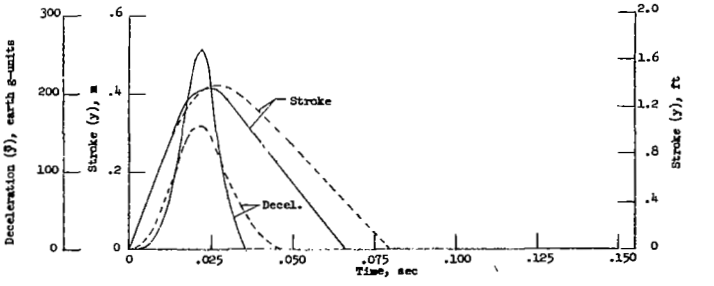

(d) Ambient pressure of 304 kN/m^2 (6350 lbf/ft^2); initial bag pressure of 304 kN/m^2 (6350 lbf/ft^2).

Figure 8.- Time histories of deceleration and stroke for the critical impact points and various ambient pressures.

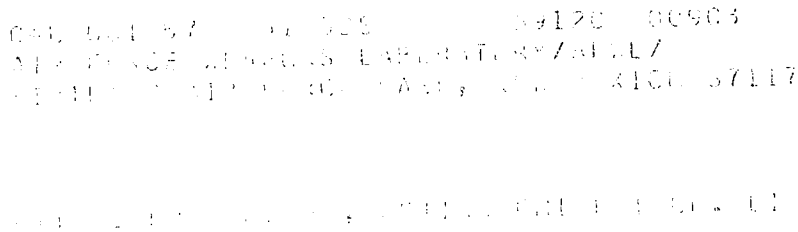

"The aeronautical and space activities of the United States shall be conducted so as to contribute . . . to the expansion of human knowledge of phenomena in the atmosphere and space. The Administration shall provide for the widest practicable and appropriate dissemination of information concerning its activities and the results thereof."

—NATIONAL AERONAUTICS AND SPACE ACT OF 1958

NASA SCIENTIFIC AND TECHNICAL PUBLICATIONS

TECHNICAL REPORTS: Scientific and technical information considered important, complete, and a lasting contribution to existing knowledge.

TECHNICAL NOTES: Information less broad in scope but nevertheless of importance as a contribution to existing knowledge.

TECHNICAL MEMORANDUMS: Information receiving limited distribution because of preliminary data, security classification, or other reasons.

CONTRACTOR REPORTS: Scientific and technical information generated under a NASA contract or grant and considered an important contribution to existing knowledge.

TECHNICAL TRANSLATIONS: Information published in a foreign language considered to merit NASA distribution in English.

SPECIAL PUBLICATIONS: Information derived from or of value to NASA activities. Publications include conference proceedings, monographs, data compilations, handbooks, sourcebooks, and special bibliographies.

TECHNOLOGY UTILIZATION PUBLICATIONS: Information on technology used by NASA that may be of particular interest in commercial and other non-aerospace applications. Publications include Tech Briefs, Technology Utilization Reports and Notes, and Technology Surveys.

Details on the availability of these publications may be obtained from:

SCIENTIFIC AND TECHNICAL INFORMATION DIVISION

NATIONAL AERONAUTICS AND SPACE ADMINISTRATION

Washington, D.C. 20546